Glycogen Dynamics in Proliferating Human Helper T Cells

Brandon Stopnicki

A Thesis

in

the Department

of

Biology

Presented in Partial Fulfilment of the Requirements

For the Degree of

Master of Science at

Concordia University

Montreal Quebec, Canada

August 2019

This is to certify that the thesis prepared

By: Brandon Stopnicki

Entitled: Glycogen Dynamics in Proliferating Human Helper T Cells

and submitted in partial fulfillment of the requirements for the degree of

Master of Science (Biology)

complies with the regulations of the University and meets the accepted standards with respect to originality and quality

Signed by the final Examining Committee:

_____   Chair
Dr. Michael Sacher

_____   External
Dr. Vladimir Titorenko

_____   Examiner
Dr. Michael Sacher

_____   Examiner
Dr. Alisa Piekny

_____   Supervisor
Dr. Peter Darlington

Approved by:

Date: _____   _____
                                   Graduate Program Director

ABSTRACT

Glycogen Dynamics in Proliferating Human Helper T Cells

Brandon Stopnicki

The immune system protects the body against infections and cancer. A type of lymphocyte called "helper T cell" plays a vital role in coordinating immune responses. Helper T cells are arguably the most important type of immune cell as they are required for almost all adaptive immune functions. T cells play a vital role in the adaptive immune system, however, very little is known about their metabolic pathways. When presented with an antigen, helper T cells proliferate, differentiate and produce cytokines. The activation of helper T cells is metabolically demanding. T cells require large amounts of glucose from their environment as they proliferate. Glycolytic by-products support rapid cell division through the building of biomass. Systematically, excess glucose is stored in the liver in the form of glycogen, but there is growing evidence that glycogen is found in non-hepatic cells as well. With an increase in glucose uptake in helper T cells, surplus must be stored for later use. Currently, there is very little knowledge on the role of glycogen dynamics in helper T cells. I hypothesized that glycogen is important in helper T cell proliferation and cytokine production. I demonstrated that isolated human helper T cells accumulated glycogen upon activation. Activated T cells accumulated a greater amount of glycogen as compared to non-activated cells ($p<0.0001$). The enzyme α-amylase, added as a control, digested glycogen and reduced the glycogen signal. Inhibition of glycogen breakdown significantly attenuated proliferation and had a trend to decrease pro-inflammatory cytokine IL-17A production in activated peripheral blood mononuclear cells. This is among the first accounts of glycogen dynamics in helper T cells. It is important to study helper T cells because they are implicated in autoimmune diseases and immune deficiencies. This newfound understanding on how helper T cells manage their metabolic needs during an immune response could aid in the development of immunomodulatory treatments.

Key words: glycogen, helper T cell, immunometabolism, proliferation

ACKNOWLEDGEMENTS

DEDICATIONS

The completion of this thesis is the product of not only my individual efforts but of the emotional investment put in by my father Daniel, my mother Miriam, and my stepmother Christina. The road was long and at times seemingly unbearable, but they never wavered in their support.

I would also like to dedicate this thesis to my sisters Zoë, Sarah and Hannah who were supportive of me throughout my studies and provided much needed support when I was feeling discouraged.

Lastly, thank you to Brooke McKee. You stood by my side throughout my entire university career and believed in me even when I did not necessarily believe in myself.

CONTRIBUTION OF AUTHORS

Figure 9 – Catalina M. Carvajal Gonczi stained and passed the sample through the flow cytometer

Figure 10 A-D – Catalina M. Carvajal Gonczi provided some of the isolated cells

Figure 11 A-D – Mayerline Dorsainvil activated, treated and stained cells

Figure 11 E & F – Catalina M. Carvajal Gonczi did the proliferation assay and ELISA for IL-17A.

Figure S1 – Chris Law and I wrote the macro in Fiji software.

Table of Contents

Abbreviations

2 NBDG – 2-(N-(7-Nitrobenz-2-oxa-1,3-diazol-4-yl) Amino)-2-Deoxyglucose

APC – antigen presenting cell

CD – cluster of differentiation

CFSE – carboxyfluorescein succinimidyl ester

DC – dendritic cell

DMEM – Dulbecco's modified eagle media

ELISA – enzyme-linked immunoabsorbent assay

FACS – fluorescence-activated cell sorting

FBS – fetal bovine serum

FIJI – Fiji is just ImageJ

G1-P – glucose 1 phosphate

G6-P – glucose 6 phosphate

GFAP – glial fibrillary acidic protein

GLUT1 – glucose transporter 1

GPI – glycogen phosphorylase inhibitor

GYG – glycogenin

GYS – glycogen synthase

IL – interleukin

MACS – magnetic-activated cell sorting

MHC – major histocompatibility complex

MS – multiple sclerosis

OXPHOS – oxidative phosphorylation

PAS – periodic acid Schiff

PBMC – peripheral blood mononuclear cell

PBS – phosphate buffered saline

PGM – phosphoglucomutase

PHA – phytohaemagglutinin

PYG – glycogen phosphorylase

PKC – protein kinase C

PMA – phorbol 12-myristate 13-acetate

RPKM – reads per kilobase of transcripts per million mapped reads

RPMI – Roswell Parks memorial institute

SD – standard deviation

SEM – standard error of the mean

Teff – effector T

Th – T helper cell

TCR – T cell receptor

TLR – toll-like receptor

TMB - 3,3',5,5'-Tetramethylbenzidine

TPM – transcripts per million

UDP – uridine diphosphate glucose

UGP - UDP-glucose-pyrophosphorylase

List of Figures

CHAPTER 1 - INTRODUCTION

In this thesis, glycogen metabolism and glycogen dynamics was explored in activated human helper T cells. In particular, my goal was to demonstrate the presence of glycogen during activation of the immune system. Additionally, I sought to test the importance of glycogen in effector function of T cells. This is amongst the first times that glycogen was observed in helper T cells. The glycogen molecule has commonly been viewed as a characteristic polymer of hepatic and muscle cells, used to systemically provide the body with glucose in times of low energy (Alberts *et al.,* 2009). We now know that glycogen storage occurs in a variety of non-hepatic cells such as immune cells (Arrizabalaga *et al.,* 2012; Hedeskov, 1968; Ma *et al.,* 2018; Quaglino *et al.,* 1962; Sadiku *et al.,* 2017; Tabatabaei Shafiei *et al.,* 2014; Thwe *et al.,* 2017). Our group contributed to this discovery by demonstrating that peripheral blood mononuclear immune cells (PBMCs) increased glycogen storage when subjected to specific types of T cell activation *in vitro* (Tabatabaei Shafiei, 2016). Here, I delved deeper into the helper T cell subset to test the hypotheses that they increased their glycogen storage when activated and that helper T cells require glycogen to proliferate properly *in vitro*. This research provided insight on a metabolic change occurring within T lymphocytes that were undergoing activation *in vitro*.

1.1 Infectious disease and the cell types of the immune system

The immune system eradicates pathogens from our body without attacking healthy tissues. Humans are made up of approximately 10^{13} human cells and 10^{14} bacterial, fungal and protozoan organisms at all times (Alberts *et al.,* 2002). While microbes outnumber human cells 10 to 1, these organisms live symbiotically as part of the microbiome and gut flora. Humans, however, frequently experience pathogenic microorganisms that could cause illness. The immune system is composed of many types of cells that work together to engulf, overwhelm and eradicate infection throughout the body. A culmination of molecular pathways mediates immune cell responses. Any slight alterations in any of these pathways could cause an inability to perform their proper immune function (McKinney and Smith, 2018; Snapper *et al.,* 1996). If our immune cells lose the ability to react to an infectious disease or gain the ability to recognize self-tissue as foreign, this results in illness or autoimmune disease, respectively (McKinney and Smith, 2018).

1.2 Adaptive Immune Response and T cell development

The adaptive immune system is comprised of B cells and T cells. T cells will be the focus of this thesis. Adaptive immune cells respond to a small fraction of the foreign pathogen called an antigen. This antigen is displayed through a transmembrane receptor called the major histocompatibility complex (MHC)-II or MHC-I. Both MHC types are located on the surface of professional antigen-presenting cells (APC), while all nucleated cells, including infected cells, express MHC-I. APCs present the antigen/MHC complex to helper T cells (identified by CD4 cell surface protein) through MHC-II. Cytotoxic T cells (identified by CD8 cell surface protein) recognize an antigen through the MHC-I receptor on the surface of antigen presenting cells and infected, cancerous or dying somatic cells. Before becoming either a cytotoxic T cell or helper T cell, the progenitor T cells from the bone marrow undergo a rigorous positive selection process. Progenitor cells travel from the bone marrow and enter the thymus as double negative for both CD4 and CD8, where they become double positive for CD4 and CD8, and leave as single positive for either one. Most autoreactive T cells are naturally killed in the thymus which provides a degree of immunological tolerance, this is called negative selection. When the cells leave the thymus, they are naïve T cells (either CD8 cytotoxic or CD4 helper). A naïve T cell is defined as a cell that has successfully undergone positive and negative selection in the thymus and is single positive for either CD4 or CD8. The naïve T cell has not encountered a foreign antigen and remains at rest. Naïve T cells that leave the thymus travel through the blood and through the lymphatic system to secondary lymphoid tissue (lymph nodes or the spleen). Positive and negative selection in the thymus are important to maintain a healthy, balanced immune system that can sense and attack foreign antigens while ignoring self-tissue (von Boehmer, 1992).

Helper T cells can cause disease in the body. Autoimmune disease occurs when a helper T cell's cognate antigen is located on self-tissue. An example of self-recognition is when helper T cells recognize and elicit a response to myelin in multiple sclerosis. These T cells recruit other immune cells such as macrophages, B cells and microglia to degrade myelin as well as the accompanying oligodendrocytes in the central nervous system (Antel *et al.,* 2018; Moore *et al.,* 2015; Salou *et al.,* 2015). In patients with type-1 diabetes, autoreactive T cells identify pancreatic β-cells as foreign and stimulate cell death. Ultimately β-cell degradation causes a reduction in insulin production in the body (Kurrer *et al.,* 1997).
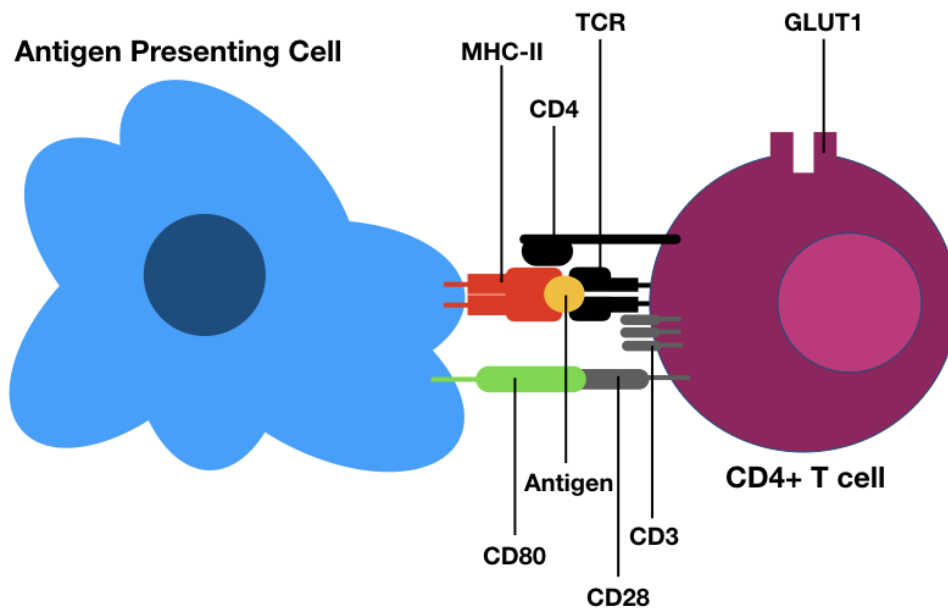
Figure 1 – Antigen presenting cell and T cell interaction.

There are multiple signals that occur when an APC interacts with a T cell. The TCR recognizes the peptide displayed on the APC by MHC. The CD4 co-receptor binds to part of the MHC allowing for the stabilization of the TCR/MHC complex and stimulates downstream activity. Intracellularly, tyrosine kinases on the tail end of CD4 phosphorylates immunoreceptor tyrosine activation motif, which is found on the intracellular tail of CD3. CD28 interacts directly with the CD80 and CD86 causing a necessary co-stimulation that starts the cell's metabolism and proliferation. CD28 is also required to increase glucose uptake through GLUT-1 and to reduce the threshold of the TCR.

Helper T cells can also cause injury within the body through cytotoxicity. Cytotoxic CD4^{+} helper T cells injure astrocytes through glial fibrillary acidic protein degradation. This reduces the ability for astrocytes to provide support for other brain cells, and prevents the astrocytes from properly repairing damaged areas (Stopnicki *et al.,* 2019). These examples of autoreactive and cytotoxic helper T cells provide insight into the importance of research that continues to uncover the inner workings of the immune system and particularly helper T cells. This understanding allows scientists to better comprehend what changes are causing disease.

1.3 Innate immunity and antigen presentation

There are two main types of immune responses: the innate response and the adaptive response. The innate response is the front-line defense of the body; some molecular components are highly conserved among metazoans. These innate cells have highly conserved receptors, such as toll-like receptors, which allow innate cells to recognize and engulf pathogens (Aderem and Ulevitch, 2000; Roach *et al.,* 2005). Professional APCs, such as dendritic cells (DCs) and macrophages, bridge the gap between the innate and adaptive immune response. APCs act mainly by internalizing antigens and then presenting them on their cell surface. Antigen presentation by APCs occurs through the MHC surface receptor. APCs, with MHC-antigen complex displayed on its surface, migrate to the lymphoid tissue to engage the adaptive immune cells by interacting with a specific matching T cell receptor (TCR). The MHC-antigen/TCR interaction provides the first activation signal for T cells (Figure 1). The MHC-II-antigen/TCR complex then requires additional interactions for T cell activation to proceed. For helper T cells, CD4 co-receptor binds to the MHC-II molecule, aiding in recognition and enhancement of the activation signalling (Artyomov *et al.,* 2010). CD28 co-receptor, found on the helper T cell, binds to CD80 on the APC, providing the second stimulatory signal for T cell activation (Figure 1). CD28 interacts directly with CD80 and CD86, causing a necessary co-stimulation that starts the cell's metabolism and proliferation.CD28 stimulates downstream protein kinase C (PKC) activation. The resulting cascade causes production of interleukin 2 (IL-2) which facilitates T cell proliferation (Linsley *et al.,* 1992). CD28 is also required to increase glucose uptake through GLUT-1 and to reduce the threshold of the TCR (Frauwirth *et al.,* 2002; Jacobs *et al.,* 2008).

1.4 T cell activation

When a naïve helper T cell encounters MHC-II-antigen complex, it may become activated. Very few such encounters will result in activation. The naïve T cell must encounter a foreign antigen/MHC that matches its unique TCR. For naïve T cells, activation occurs through the interaction of the TCR complex and co-stimulatory transmembrane protein receptor CD28 (Bluestone, 1995; Linsley *et al.,* 1992). The TCR variable region identifies the MHC-bound antigen, and the CD3 transmembrane molecules cause the intracellular cell signalling cascade. CD3 is present on all T cells and is a common extracellular identifier. Together, the TCR/MHC-antigen complex and the CD28/CD80 interaction causes a cascade of reactions that result in the naïve T cell becoming an activated effector T cell (Smith-Garvin *et al.,* 2009) When the TCR recognizes its cognate antigen the T cell starts to divide, making clones of itself. This process, called clonal expansion, increases the population of cells specific to this one antigen.

T cell activation can be simulated in the laboratory in a variety of different ways (Figure 2). *In vitro*, the TCR can be stimulated by adding anti-CD3 to the cell culture. A heterogenous population of immune cells derived from PBMCs can be activated *in vitro* by using the phorbol 12-myristate 13-acetate (PMA). PBMCs are an isolated group of cells from whole blood that contain an array of immune cells, a large proportion of which are T lymphocytes. PMA bypasses the CD28 co-receptor by crossing the cell membrane and directly activating PKC. PMA has a similar structure to diacylglycerol, which allows it to activate PKC. Another method for T lymphocyte activation is through the addition of soluble (free floating) polyclonal antibodies that are specific for CD3 or CD28. It is thought that the soluble antibodies are presented to the T lymphocyte by monocytes in cell culture. Monocytes are a component of the PBMC suspension and can differentiate into macrophages or dendritic cells. Similar antibodies can also be fixed to a plastic surface in the form of micro-beads (dynabeads) which is most effective in activating helper T cells that are cultured without PBMC support. Measuring T cell activation usually involves measuring IL-2 and expression of CD69 on the cell surface (Kamphorst *et al.,* 2017; Saparov *et al.,* 1999). T cell proliferation is primarily induced by autocrine and paracrine IL-2 signalling. IL-2 promotes the T cell through the cell cycle by upregulating cyclin proteins (Appleman *et al.,* 2000; Modiano *et al.,* 1994) whereas CD69 is the first notable receptor to be translocated to the membrane upon activation and is used as a marker for T lymphocyte activation (Cibrián and

Sánchez-Madrid, 2017; Ziegler *et al.,* 1993). IL-2 and CD69 are also indicators of activation *in vitro*.
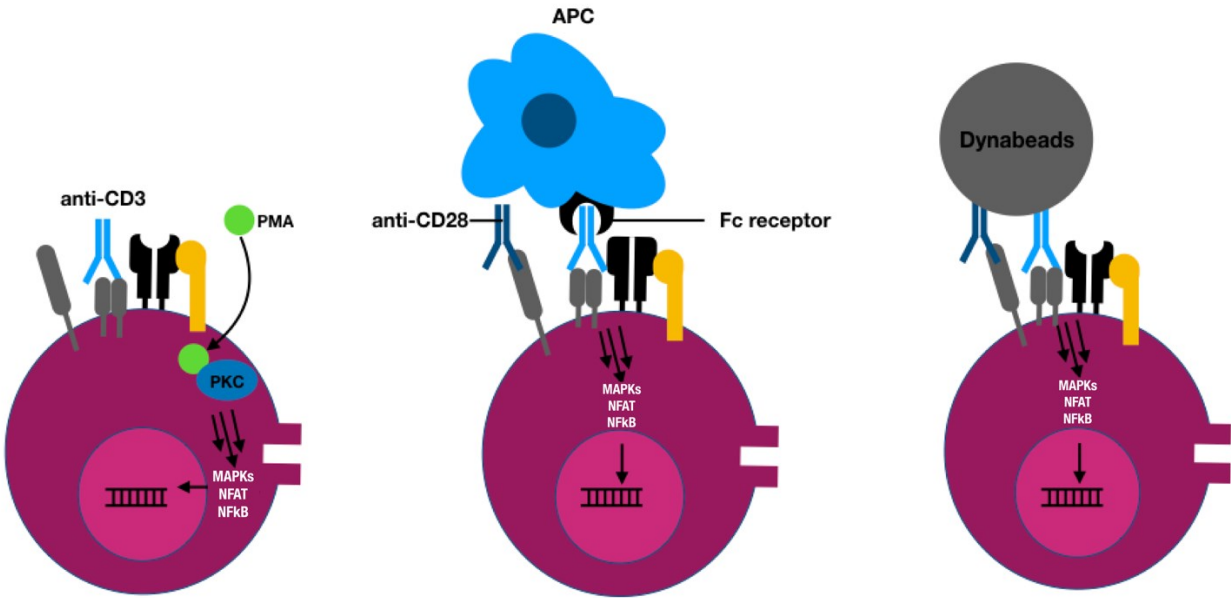
Figure 2 – Activation of lymphocytes using different methods *in vitro*

In the laboratory, T cell activation can be simulated with a variety of methods. **A)** PMA crosses the plasma membrane directly and interacts with PKC to cause a downstream activation cascade. **B)** Soluble anti-CD3 and anti-CD28 is presented to the lymphocytes by monocytes, therefore crosslinking the TCR. **C)** The dynabeads can be used without the need for APCs and are optimal for activating isolated T lymphocytes *in vitro*.

Proliferating T lymphocytes can be seen clustering together and can be monitored using microscopy techniques. An increase in cell area is an indicator of activation (Iritani et al., 2002; Rathmell et al., 2003). Helper T cell proliferation also can be monitored *in vitro* using dyes that decrease in intensity after each generation such as carboxyfluorescein succinimidyl ester (CFSE; described further in the materials and methods section). T cells that receive all of the necessary signals (CD3, CD28 and IL-2) can proliferate, and differentiate in order to more specifically target the threat.

Mature helper T cells are necessary for both B cell activation, in the secondary lymphoid tissue, and propagation of the complement system (Crotty, 2015). Additionally, helper T cells release a slew of cytokines to recruit other immune cells, such as macrophages and neutrophils, to the site of infection (Franciszkiewicz *et al.,* 2012). When the threat dissipates, helper T cells either die off or become memory T cells. Memory helper T cells can be identified by their exclusive expression of CD45RA. Memory cells can respond more rapidly the next time the same pathogen invades the body (Baaten *et al.,* 2010). The helper T cell's ability to cover a variety of functions makes them crucial to the immune system.

1.5 The importance of CD28 co-stimulation

Stimulation of helper T cells and the expansion of their antigen-specific population occurs through their interaction with professional APCs. In addition to the MHC/TCR interaction, CD80 and CD86 on the APC binds to CD28 on the helper T cells. This stimulation decreases the threshold of the TCR activation (Esensten *et al.,* 2016). Co-stimulation is critical for controlled activation and increased proliferation of T lymphocytes (Kündig *et al.,* 1996). CD28 co-stimulation will increase cell surface trafficking of glucose transporter GLUT1 (encoded by *SLC2A1* gene) to facilitate glucose uptake in T lymphocytes (Frauwirth et al., 2002; Jacobs et al., 2008; Macintyre et al., 2014). The CD28 stimulation pathway is necessary to increase the effectiveness of current cancer immunotherapies. For example, Kamphorst *et al.,* (2017) conducted a study exploring an immunotherapy technique that used a monoclonal antibody against PD-1 on exhausted cytotoxic T cells in attempts to rescue them. They found that in a tumor microenvironment, infiltrating CD8 T cells are suppressed by the tumor through their interaction with PD-1. In their study, they used a murine model of lifelong chronic lymphocytic choriomeningitis virus infection to demonstrate that the activation, proliferation and rescue of infiltrating cytotoxic T cells from the tumor

microenvironment, relied on CD28 co-stimulation (Kamphorst *et al.,* 2017). These studies suggested that glucose metabolism is mediated by CD28 co-stimulation and is a vital aspect of maintaining continued energy production, proper function and maintenance of T lymphocytes in proliferative states.

1.6 Immunometabolism

Metabolites such as glucose are a limiting factor in sustaining a strong immune response. During division of all somatic cells, large quantities of building blocks are necessary for DNA synthesis, membrane biosynthesis and energy production (Alberts et al., 2009). Activated T lymphocytes require these building blocks to maintain their proliferative state (van Stipdonk *et al.,* 2003). Within two hours of activation with anti-CD3 and anti-CD28 antibodies *in vitro*, there is an increased expression of the GLUT1 to support an increase in glucose uptake. The importance of glucose metabolism was shown by using a knockout of *GLUT1* gene in mice, which impairs T lymphocyte activation and proliferation (Macintyre *et al.,* 2014). While most interphase and G_0 cells use oxidative phosphorylation (OXPHOS) to satisfy their metabolic needs, proliferating cells will use both OXPHOS and aerobic glycolysis. While the efficiency of ATP production is much lower in glycolysis, glucose is typically not rate-limiting and permits carbon to be shuttled to biomass production (Rashida Gnanaprakasam *et al.,* 2018). There is evidence that proliferating helper T cells favor a biosynthetic metabolic program through aerobic glycolysis (Bental and Deutsch, 1993; Dumitru *et al.,* 2018). Naïve T cells may circulate in the blood and lymph without ever coming across an antigen and will use OXPHOS to provide ATP for regular cell processes (Klein Geltink *et al.,* 2018). A naïve T cell that comes in contact with an antigen-MHC complex will shift its metabolism towards biosynthetic pathways to satisfy the bioenergetically demanding process of proliferation and clonal expansion (Heiden *et al.,* 2009; Lunt and Vander Heiden, 2011). The final product of glycolysis, pyruvate, is converted into lactate. This process, called the Warburg effect, was first described in cancer cells by Otto Warburg (Weinhouse *et al.,* 1956) (Figure 3). Aerobic glycolysis also supports an increase in inflammatory cytokine production, which is important for immune activation and is a hallmark of helper T cell activity (Menk *et al.,* 2018). Although aerobic glycolysis is not necessarily efficient in producing ATP, it provides precursors to make amino acids, pyrimidines and purines (Berg *et al.,* 2010).

14
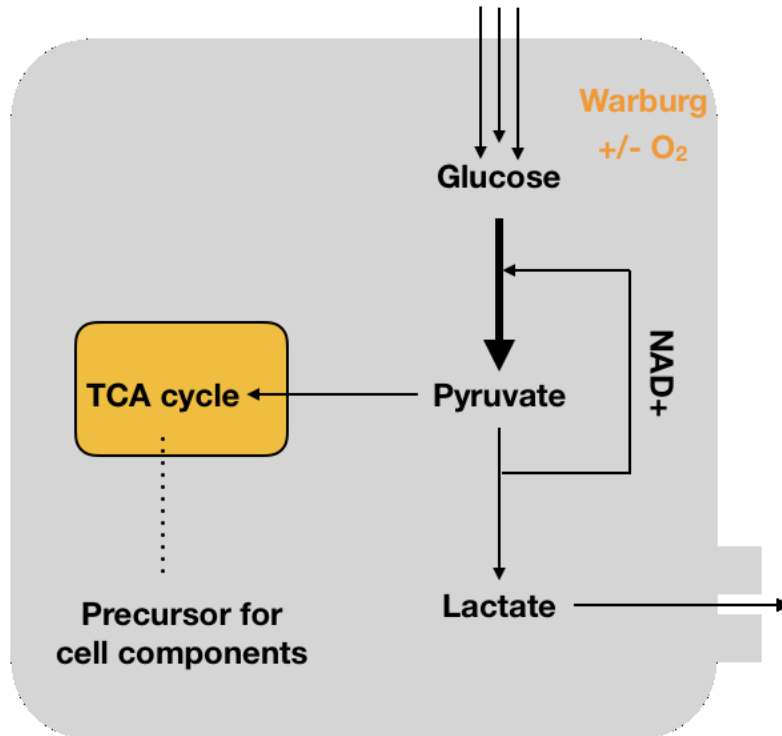
Figure 3 – Increased glycolysis (Warburg effect)

Activated, highly proliferative cells often undergo a metabolic shift towards the use of glycolysis (even in the presence of oxygen) to produce lactate. This is called the Warburg effect. Glucose is broken down to produce pyruvate and lactate. Lactate is excreted from the cell, while the NAD^+ that was reduced is used again in glycolysis. Pyruvate also has the ability to enter the TCA cycle. While ATP production is minimal compared to OXPHOS, biosynthetic precursors are made to support a shift towards anabolism instead of catabolism.

Pentose phosphate pathway and serine biosynthesis pathway intermediates are used to replicate DNA, synthesize phospholipids for new cell membranes and translate proteins necessary for rapid cell division (Wang *et al.,* 2011). Glucose can also be converted into acetyl-CoA for lipid synthesis (DeBerardinis *et al.,* 2008). Utilizing glucose as a precursor for substrate production is the backbone for an efficient and uninterrupted T lymphocyte expansion (Jacobs *et al.,* 2008).

An influx of metabolites is required to orchestrate T lymphocyte proliferation. Helper T cell proliferation relies on glucose and glutamine for energy and for building biomass. Glucose influx creates an environment within the cell that is hypertonic to the surrounding medium (blood or lymph). Therefore glucose uptake at these high rates can be osmotically unstable for the cell and excess glucose must be stored in a way that is efficient for proliferating helper T cells.

1.7 Glycogen as a source for glucose storage and more

Glycogen is a branched polymer of glucose used for energy storage in a wide variety of organisms (Roach et al., 2012). When energy levels are high, excess glucose is stored in the form of glycogen, which is triggered through the insulin pathway (Fadista *et al.,* 2014). In contrast, in times of low energy, glucagon and epinephrine signal glycogen breakdown which then feeds glucose into metabolic pathways to produce energy and other by-products (Carroll *et al.,* 1956). To form glycogen, glucose is first phosphorylated to make glucose 6-phosphate (G6-P). G6-P can also be derived through gluconeogenesis, which is controlled by the enzyme phosphoenolpyruvate carboxylase-1 (Figure 4). G6-P will need to be converted to glucose 1-phosphate (catalyzed by Phosphoglucomutase; *PGM*) and then UDP-glucose (catalyzed by UDP-glucose-pyrophosphorylase; *UGP*) before glycogen polymer synthesis (glycogenesis) can begin. Glycogenin (*GYG1*) proteins initiate polymerization of the first two glucose monomers, through α1-4 glycosidic linkages, which are then extended by the action of glycogen synthase (encoded by *GYS1* and *GYS2*; Figure 4 and 5). The glycogen branching enzyme causes the formation of α1-6 linkages (Figure 5). This enzymatic pathway results in a highly branched polymer that has been reported to have a molecular mass of $\sim10^7$ kDa with a diameter of $\sim$44nm (Goldsmith *et al.,* 1982). Glycogen polymers can be seen as rosette-like particles through electron microscopy and are dark purple granules when subject to periodic acid Schiff (PAS) staining (Drochmans, 1962; Quaglino *et al.,* 1962; Tabatabaei Shafiei, 2016). Breakdown of glycogen (glycogenolysis) is

16
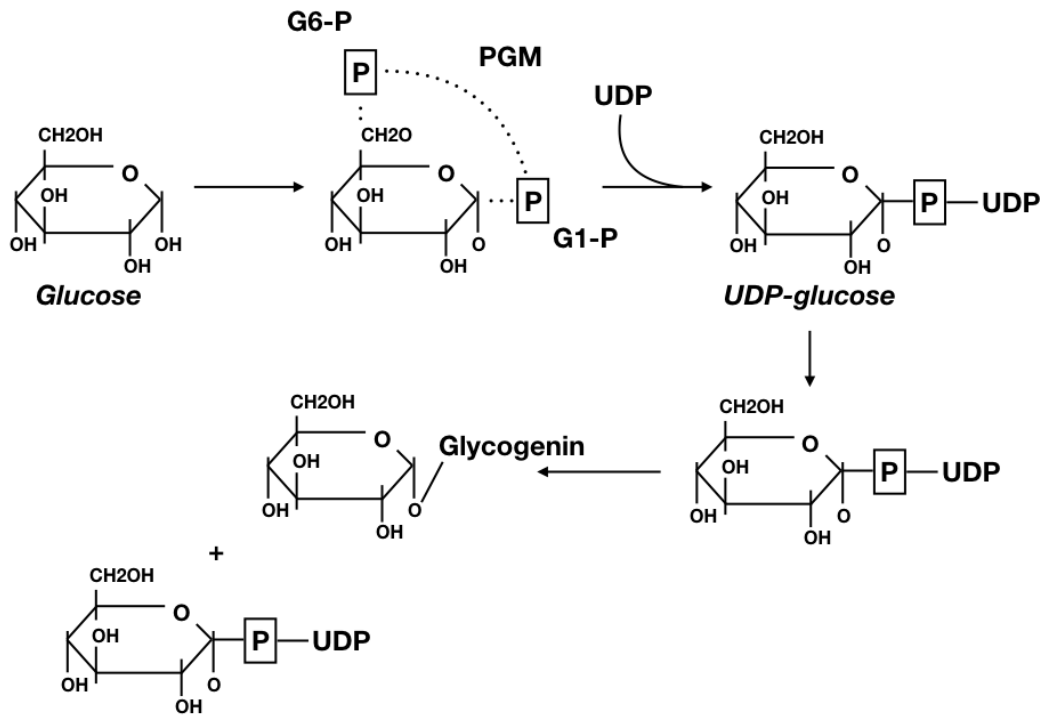
Figure 4 – Glycogen synthesis starting from glucose

This schematic describes the synthesis of a new glycogen polymer starting with glucose. Glucose is first converted to G6-P. This can be derived as shown here by a glucokinase or directly from gluconeogenesis. PGM enzyme catalyzes the phosphate change from the 6C to the 1C on the glucose monomer. Addition of Uridine Diphosphate is catalyzed by UGP enzyme to form UDP-glucose. Glycogenin acts as a primer to bring the first two UDP-glucose monomers together to form a short chain glycogen dimer. GYG is needed only until the chain reaches about eight glucose monomers. Addition of consecutive monomers and branches are catalyzed by glycogen synthase and glycogen branching enzyme respectively. This figure was created by Brandon Stopnicki using Berg *et al.,* 2010 as reference.
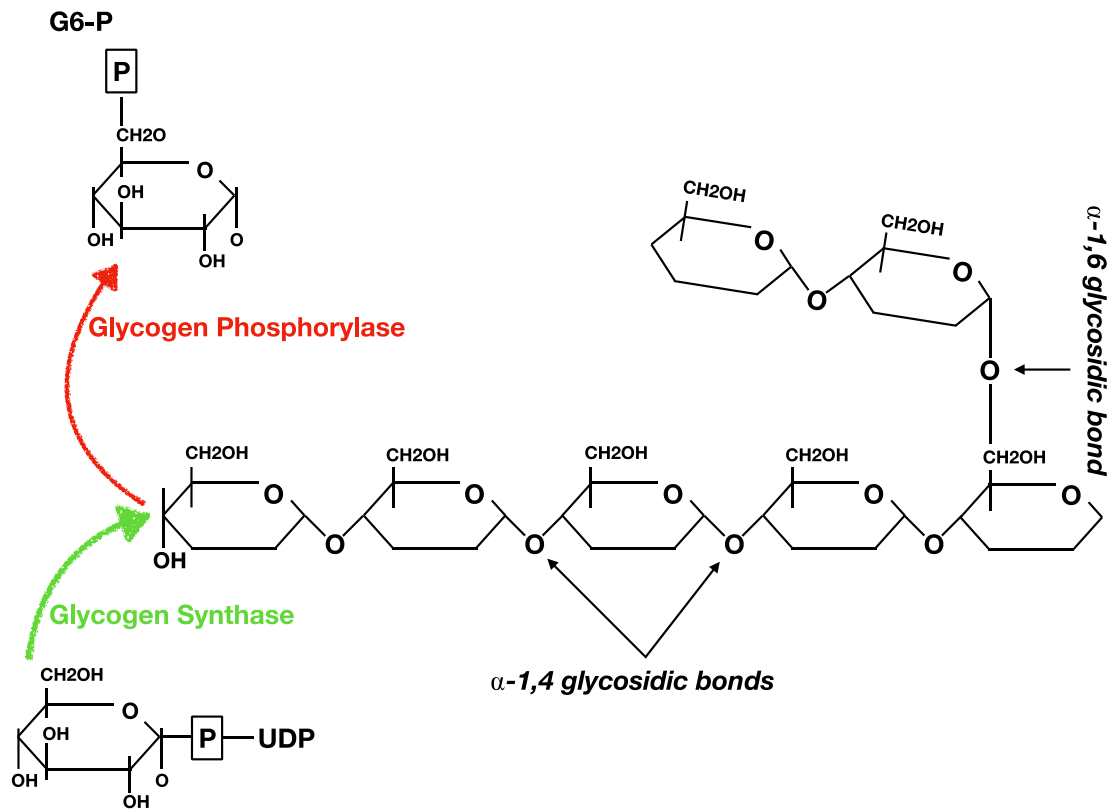
Figure 5 – Schematic of glycogen bonding and branching pattern

Glycogen synthase, encoded by the *GYS* gene, adds UDP-glucose monomers to the growing chain at the 4C hydroxyl, forming α1,4 glycosidic bonds. Glycogen phosphorylase breaks down glycogen into G1P, which can then be used in a variety of pathways after being converted to G6P. Addition to the 6' C is carried out by Glycogen branching enzyme, which makes α1,6 glycosidic bond and is encoded by *GBE1* gene. Glycogen phosphorylase removes residues until there is a chain of 4 glucose monomers. The glycogen debranching enzyme (encoded by *AGL* gene) must break the α1,6 glycosidic bond before the phosphorylase can continue. This figure was created by Brandon Stopnicki using Berg *et al.,* 2010 as reference.

caused by glycogen phosphorylase which de-polymerizes α1-4 linked glucose monomers followed by glucosyltransferase and amyloglucosidases. α-amylase can also be used to break down the glycosidic linkages in glycogen. This is followed by conversion of α1-6 positions into α1-4 linkages for removal by glycogen phosphorylase which is encoded by the gene *PYG* (isoforms for *PYG* include, *PYGB, PYGL* and *PYGM*) (Berg *et al.,* 2010). In humans and other mammals, glycogen is typically stored and manufactured in the liver, however glycogen has also been found in non-hepatic tissues such as muscles, brain cells and immune cells.

Glycogen is an important metabolic regulator for a variety of non-hepatic cells. In astrocytes (neuroglial cells), glycogen is converted to glucose which is then processed into l-lactate to fuel neurons and other glial cells (Suzuki *et al.,* 2011). Lactate, and consequently glucose, is important for astrocytes since they shuttle this lactate to neurons. Glucose uptake in reactive astrocytes, induced by oxygen-glucose deprivation, was monitored using the fluorescent glucose analog 2-(*N*-(7-nitrobenz-2-oxa-1,3-diazol-4-yl) amino)-2-deoxyglucose (2-NBDG). It was determined that glucose uptake was increased in reactive astrocytes (Chen *et al.,* 2015). Surplus of glucose is stored as glycogen in astrocytes as a "energy buffer" in case of low-glucose levels (Brown *et al.,* 2003; Waitt *et al.,* 2017). Glycogen impairment in astrocytes negatively affects the central nervous system. Specifically, impairments in glycogen dynamics have been implicated in processes involving memory formation in the hippocampus and its decreased content may contribute to a depression-like behaviour in rats (Hertz and Chen, 2018; Horvat *et al.,* 2017; Magistretti and Allaman, 2018; Newman *et al.,* 2011; Zhao *et al.,* 2017). Besides providing a supply for lactate, glycogen also provided precursors to form glutamate, which is an important neurotransmitter (Araque *et al.,* 2014; Savtchouk and Volterra, 2018; Zhang *et al.,* 2014). While there is substantial evidence that glycogen is important in glial cell functionality, glycogen is also required in other non-hepatic cells.

Glycogen has been found to modulate the function of certain immune cells. An increased glycogen storage in neutrophils is linked to an excessive innate immune response in *Phd2*-deficient mice. Blocking glycogenolysis with a glycogen phosphorylase inhibitor (GPI), caused an increase in the apoptosis rate of neutrophils (Sadiku *et al.,* 2017). An overactive neutrophilic response is a hallmark of autoimmune conditions like asthma, allergy, lupus and rheumatoid arthritis (Courtney *et al.,* 1999; Fu *et al.,* 2013; Wipke and Allen, 2001). In PBMCs, it has been demonstrated that glycogen accumulates after 24-hours and was sustained over 72 hours with anti-CD3/anti-CD28

(Tabatabaei Shafiei, 2016). Most of what is known about glycogen in lymphocytes was discovered in the 1960s (Quaglino *et al.,* 1962, 1964), when it was demonstrated that phytohaemagglutinin (PHA)-activated lymphocytes had a higher glycogen concentration than that of resting cells. They showed an increase of glycogen granules in immature pro-lymphocytic and blast cells, but they were not able to conclude this as a sufficient method for cancer diagnosis due to the contradictory findings of others (Jones *et al.,* 1962; Leder and Donhuijsen, 1978). This left the topic of glycogen dynamics in healthy human T lymphocytes as a gap in the literature. Until recently, very little research into the biological relevance of glycogen storage and its use in immune cells had been conducted. Recent publications display evidence that glycogen increases in activated T lymphocytes and that glycogen plays important regulatory role in dendritic cells and cytotoxic CD8 T cells (Ma et al., 2018; Tabatabaei Shafiei, 2016; Thwe et al., 2017). There is a lack of data implicating glycogen as a requirement for helper T cell function.

1.8 Experimental directions of thesis

Using helper T cells, I explored the dynamics of glycogen storage in conditions where the T lymphocytes are activated. There is overwhelming data showing that in proliferating helper T cells an increase in glucose metabolism is crucial (Eiraku *et al.,* 1998; Frauwirth *et al.,* 2002; Greiner *et al.,* 1994). The depletion of glucose during clonal expansion is not only a problem for energy availability but also for biomass accumulation. Glycogen is a means for glucose to remain constant even in low glucose environments. Inhibition of glycogenolysis or glycogenesis would be detrimental to the proliferation of helper T cells. A broader comprehension of the key cells in the adaptive immune response will help scientists better understand current therapies and to conceptualize future treatments for diseases. Helper T cells are arguably the most important adaptive immune cell; therefore, evidence of glycogen storage in these cells is important in contributing to our understanding of the immune systems' functionality as a whole as well as for disease pathology.

CHAPTER 2 – HYPOTHESIS AND AIMS

2.1 Hypothesis

Glycogen accumulates in activated helper T cells and is necessary for T lymphocyte proliferation.

2.2 Aims

Below is indicated the manner in which I will test the overarching hypothesis.

2.2.1 Aim 1

Determine whether or not glycogen is found in helper T cells and if its amount changes when activated.

2.2.2 Aim 2

Determine if T lymphocyte proliferation is affected when glycogen metabolism is inhibited in T lymphocytes.

2.2.3 Aim 3

Determine if the expression of genes involved in the glycogen pathway is altered in helper T cells due to cell activation.

CHAPTER 3 - MATERIALS AND METHODS

3.1 PBMC isolation and participants

The project was approved by Concordia University Ethics Review board (certificate # 30009292). Participants were determined to be healthy individuals by self-reporting. Prior to the blood draw, participants were asked to sign a consent form. The consent form outlined the risks of giving blood, which included possible bruising and light-headedness. Blood was drawn by a phlebotomist through venipuncture and into anti-coagulant blood-collection tubes. All manipulations of PBMCs were done in a biosafety cabinet. PBMCs were isolated using a density gradient centrifugation technique with Ficoll-Paque PLUS (GE Healthcare Biosciences) as described previously (Tabatabaei Shafiei *et al.,* 2014). PBMCs can be found in the buffy coat layer that resulted from the centrifugation technique. A buffy coat is the cloudy white layer containing mononuclear lymphocytes that excludes red blood cells, platelets, neutrophils, and other polymorphonuclear cells. PBMCs were counted using trypan blue solution (ThermoFisher Scientific) and then stored at $2x10^7$ cells/aliquot in -80℃. Trypan blue counting was also used to assess viability. Trypan solution was added to equal volume of PBMCs and mixed. The suspension was then transferred to a haemocytometer and analyzed with the Leica DM2000 microscope. Dead cells took up trypan dye and appeared blue. Percent viability was calculated using Formula 1 (see Appendix). Once cells were counted and viability was assessed, the cells were placed in culture.

3.2 Cell culture conditions, activation and treatments

PBMCs were cultured in sterile round bottom 96-well plates with complete media, which included Roswell Park Memorial Institution (RPMI) 1640 medium, 11mM D-glucose, 10% fetal bovine serum (FBS), 1mM penicillin/streptomycin and 1mM L-glutamine. D-glucose is in excess in the complete RPMI (11mM) whereas the physiological blood glucose levels are around 5.5mM (Güemes *et al.,* 2016) For figure 6, cells were cultured in 24-well flat bottom culture plates to facilitate imaging. PBMCs were activated with phorbol 12-myristate 13-acetate (PMA; 2ng/mL; Sigma-Aldrich) and anti-CD3 (0.1μg/mL; eBioscience). There is evidence that PMA can activate PKC directly (Robinson, 1992). PMA is not a specific activator of T lymphocytes which suggests that is will activate most cell types within the PBMC suspension. Therefore, PBMCs were also

activated with specific activator of T lymphocytes, monoclonal anti-CD3 and anti-CD28 (eBioscience; $0.1\mu g$/mL each). Cells were incubated at 37℃ with 5% CO_2 for 24 and 48-hours. Isolated helper T cells were activated with anti-CD3/anti-CD28 dynabeads (ThermoFisher Scientific). Dynabeads were washed prior to use with recommended buffer (phosphate buffered saline (PBS), 0.1% BSA and 2mM EDTA pH 7.4). Prior to downstream manipulation, the cell suspension was removed. The plate was placed on a magnet to ensure the dynabeads stuck to the bottom of the wells and were not removed with the cell suspension.

To inhibit glycogen breakdown, PBMCs were cultured with GPI (BAYU6751, $0.5\mu M$) for 48 hours before being harvested and stained with PAS. PBMCs were cultured using complete RPMI media with low serum (1% FBS). The effect of GPI on proliferation was assessed through flow cytometry.

For astrocyte work, foetal human brain tissue was provided by the Albert Einstein College of Medicine (Bronx, NY, USA) in accordance with Albert Einstein College of Medicine and McGill University institutional review boards. Astrocytes from the aforementioned tissue were isolated at the Montreal Neurological Institute's Neuroimmunology unit. All experiments involving astrocytes were done in the neuroimmunology unit at the Montreal Neurological Institute under the supervision of Dr. Luke Healy and his staff. Astrocyte-enriched cultures were prepared by obtaining a dispersed cell suspension from the foetal brain tissue by trypsinization and mechanical disruption. The cells were then cultured in Dulbecco Modified Eagle Media (DMEM) with 10% foetal bovine serum (FBS), pen/strep, L-glutamine, with at least three passages before use. The astrocytes were seeded on thermanox coverslips (ThermoFisher Scientific) in 24-well plates and used upon confluency. Astrocytes were made reactive with the addition of cytokine IL-1β (1ng/mL) and then incubated for 24-hours at 37℃ with 5% CO_2.

3.3 Glycogen visualization

3.3.1 2-NBDG

Glycogen was visualized in helper T cells and PBMCs through both fluorescence and histological staining. Activated PBMCs were pulsed with $50\mu M$ of 2-(N-(7-nitrobenz-2-oxa-1,3-diazol-4-yl) amino)-2-deoxyglucose (2-NBDG; ThermoFisher Scientific) for 2 hours in D-glucose-free RPMI. Glucose-free RPMI was used to prevent glucose uptake competition with 2-

NBDG. 2-NBDG is a fluorescent glucose-analog that is commonly used to study glucose uptake. Cells were then washed and replaced with complete D-glucose RPMI (pen/strep, L-glutamine and 10% FBS). Pulsation was crucial since, once 2-NBDG enters the cell, it becomes phosphorylated and cannot exit causing accumulation which is potentially cytotoxic for the cell. The optimal concentration and time of pulsation was determined using Jurkat T cell line by titration of increasing concentrations of 2-NBDG from 10μM-500μM. Cells were washed with ice-cold 1X-PBS. PBMCs were similarly pulsed with $50\,\mu$M of 2-NBDG for 1-hour in glucose-free RPMI (10% FBS). The PBMCs were washed and media was replaced with D-glucose complete RPMI (10% FBS) for 48-hours. Both Jurkat T cells and PBMCs were then visualized with the Leica DMi-6000B fluorescent microscope with excitation/emission maxima ~465/540nm, respectively. Images were processed in Fiji software (Fiji is just ImageJ). Glycogen granules in PBMCs, muscle and human pluripotent stem cells (Chen *et al.,* 2015a; Tabatabaei Shafiei *et al.,* 2014), have a distinct punctate morphology, therefore glycogen was qualitatively defined through its morphological features.

Glycogen was visualized in human foetal astrocytes using 2-NBDG. Astrocytes were starved of glucose for a minimum of 1-hour prior to 2-NBDG treatment. 2-NBDG (25μM) was then added to astrocyte cultures in 24-well plates for 1 hour with glucose-free DMEM (10% FBS). The cells were then washed (1XPBS) and media was replaced with D-glucose DMEM (10% FBS) for 24-hours. Cells were fixed with 4% paraformaldehyde for 10-15 minutes at room temperature. Astrocytes were then stained with Hoechst (blue) and Cy3-GFAP (Sigma-Aldrich). For Cy3-GFAP intracellular staining, astrocytes were permeabilized in 0.3% triton X-100. Images were obtained on an inverted epi-fluorescent microscope at the Centre for Microscopy and Cellular Imaging (CMCI) located at Concordia University (Leica DMi-6000B). Resulting images were processed using Fiji software.

3.3.2 Periodic acid Schiff's histological stain

Glycogen was also visualized using PAS reaction as described previously with small modifications (Tabatabaei Shafiei *et al.,* 2014). Periodic acid oxidized the C-C bond in carbohydrates that have a free hydroxyl group. This resulted in dialdehydes which then react with the Schiff's reagent forming a magenta-coloured complex that was monitored with light microscopy techniques and quantitatively analyzed with Fiji software (described below). The

periodic acid selectively oxidizes polymers of high molecular weight and not low molecular weight water soluble monosaccharides such as glucose.

PAS staining was done on both PBMCs and isolated helper T cells. PBMCs and isolated helper T cells were fixed with 4% paraformaldehyde prior to staining. Staining was done in 96-well V-bottom culture plates to minimize cell loss that occurred when staining directly on a microscope slide. Cells were suspended in periodic acid and then washed twice with ddH$_2$O. After the first washing step, the cells were resuspended in Schiff's reagent and incubated in the dark for 15 minutes. Cells were washed 4 times. Each wash step required 30 seconds of agitation in ddH$_2$O. Cells were then placed on a glass slide and left to air dry. Once the slides were dry, a drop of toluene mounting media (Permount) was added on top of the cells and a coverslip was placed over it. Each slide was then sealed with clear nail polish. Images were taken using a Nikon Eclipse TiE and Leica DM2000. Resulting images were processed using Fiji software.

3.3.3 Image processing

Images of PBMCs and helper T cells that were stained with PAS were captured on a Nikon Eclipse TiE. 5 pictures were taken, in duplicates, for each slide (representing one participant sample). The bright field images were opened in Fiji software and the mean signal intensity and area of each cell was measured. For each replicate all the cells in the 5 images were measured for both signal intensity and for cell size measurements. Not all cells had the same background (inside the cell) staining intensity. Certain cells stained bright pink over the entire cell area. Only cells that had a faint pink background were chosen for analysis. This bias was introduced to eliminate the cells that had outlier levels of signal intensity.

The mean signal intensity was measured using Fiji software. A macro (Figure S1) was designed that did the following. The image contrast was enhanced, and the green channel was split out. The green channel has the most contrast, which is why this channel was chosen. The image was blurred to hide small artifacts such as cell debris. Lastly, the macro told Fiji to threshold the images to find areas above 1500 pixels in size, which we can assume are cells. The cell areas are selected as regions of interest and measured on the grey scale for mean pixel intensity. These areas were not always cells, which is why each image was monitored for errors by me seeing that the region of interest was not debris or background staining. For cells at rest, the threshold was often too high and therefore the cells had to be selected by hand.

3.4 Amylase treatment

Amylase powder (Sigma-Aldrich) was reconstituted as per manufacturer's instructions and as described previously (Tabatabaei Shafiei, 2016). Helper T cells were activated with dynabeads and then fixed with 4% paraformaldehyde. The cells were then treated with α-amylase prior to being stained with PAS to digest glycogen. This condition was designated as the negative control. The helper T cells were incubated with amylase solution for 10 minutes. Cells were washed with 1X-PBS and re-suspended in complete RPMI. These cells were subjected to glycogen visualization techniques as described above.

3.5 CD4$^+$CD3$^+$ T lymphocyte isolation

Using EasySep Human CD4$^+$ T cell Isolation Kit (StemCell technologies), helper T cells (defined through the surface proteins CD4$^+$CD3$^+$) were isolated from PBMCs. This process is done through immunomagnetic negative selection by adding (according to supplier's instructions) antibody cocktail (50μL/mL) and magnetic spheres (50 μg/mL) to PBMCs in suspension at 5x10^{7}cells/mL in the recommended media (2% FBS, PBS, 0.2% EDTA). The negative selection antibody kit removed cells positive for CD8, CD14, CD15, CD16, CD19, CD36, CD56, CD123, TCR γ/δ and CD235a. Magnetic spheres were then added to the suspension. The solution was added to a magnetic column and the non-CD3+CD4+ were taken out of solution by the magnetic. The flow through was poured off and contained helper T cells. Purity was assessed via flow cytometry (Figure 9).

3.6 Flow cytometry

Purified helper T cells were labeled with anti-CD4 (PerCP) and anti-CD3 (APC) to determine the effectiveness of the negative selection. Each cell is represented on the 2D-histogram by a point. Side scatter (x-axis) represents cell complexity. A laser was shot at each cell individually as it passed through the fluidics section of the flow cytometer. Laser light hit the intracellular components, was scattered and then picked up by a specialized receptor. Forward scatter (y-axis) represents cell size. The light from the laser that is not shielded by the cell makes it to the receptor opposite the laser. Dead cells or cell debris are often small and are dense therefore

resulting in low light scatter (side scatter). Live cells were gated based on their size and complexity. Of the live lymphocytes, the double positive population ($CD4^+CD3^+$) was used for analysis and considered helper T cells. For the proliferation assay, CFSE was recorded via channel for FITC (λ=495nm). The dye entered the cell as CFDA-SE and was first converted to CFSE. CFSE then covalently labels long-lived proteins inside the cell (CF-protein). Each cell division resulted in the fluorescent signal diminishing by half, since the daughter cells obtained half the material of the original cell when it divided. This way, the extent of proliferation was quantitatively determined by the rate in which the signal degraded over time. The flow cytometry data was analyzed using FlowJo software (TreeStar).

3.7 Enzyme-Linked Immunosorbent Assay (ELISA)

ELISA was used to measure the concentration of released cytokine IL-17A. Standard sandwich ELISA was used (eBioscience). The steps were done according to manufacturer's instructions. Capture antibody was incubated in a 96-well plate overnight for it to be stuck to the plate. The plate was washed and then blocked with assay diluent (10% FBS in 1XPBS) to eliminate any unspecific binding of the capture antibody. Blocking is followed by a series of washing steps (with wash buffer: PBS-tween). The samples were diluted and added to the wells, then incubated to let them bind to the capture antibody. Incubation was followed by a series of washes with wash buffer. The working detection antibody was added to the wells, which is specific to a portion of the protein of interest. The detection antibody is conjugated with horseradish peroxidase (SAv-HRP). Another series of washes were done before adding substrate. HRP reacted with 3,3'5,5'-tetramethylbenzidine (TMB) substrate to a form coloured product. The reaction was stopped using sulfuric acid (2N) yielding a yellow colour. The absorbance was read at 450nm (yellow) and 570nm (used for wavelength correction). Wavelength correction was used to remove background emissions from the reading. Absorbance was proportional to the amount of protein added to the well.

3.8 RNAseq analysis

RNAseq data was obtained from GEO public NIH database. The authors of the datasets carried out the RNA sequencing in the following way: Total RNA from human helper T cells was

purified and converted into cDNA. Helper T cells were isolated from venous blood similarly to that of this thesis. Methods for RNA library formation and sequencing can be found in Gate *et al.,* 2018, and Komori *et al.,* 2015. The authors purified total RNA and converted it into cDNA. The RNA was selected for size using electrophoresis and then libraries were amplified through PCR. Cluster generation and RNA sequencing was done using an Illumina HiSeq (for Gate *et al.,* 2018) and Illumina GAIIx (for Komori *et al.,* 2015). Sequenced reads were aligned to a reference genome (hg18 and hg19) and analyzed as described in the methods section of their manuscript (Gate *et al.,* 2018 and Komori *et al.,* 2015). TPM (Gate *et al.,* 2018) and RPKM (Komori *et al.,* 2015) formulas were used to express the data. TPM and RPKM (also FPKM, RPM and raw read counts could be used) are both expression units that provide a means to express the abundance of a transcript within a sample. While there are benefits for using either RPKM or TPM to express RNAseq data TPM has arisen as the more reliable method. The main differences between RPKM and TPM are that in TPM formula, normalization for gene length occurs first where RPKM normalizes for sequencing depth first. The outputs for the sum of all the TPMs in the sample are the same, making them easily comparable between samples (Formula 3). For different RPKM outputs, the proportions may be different between samples making them potentially more difficult to compare. Fold-change for the expression levels of genes involved in glycogen dynamics was determined for each participant. Error bars represent sequencing runs performed (n=6 for both studies). Raw data can be found using accession numbers GSE59860 and GSE86888 for Komori and Gate manuscripts, respectively.

3.9 Statistics

Statistical analysis with multiple comparisons was done using a one-way ANOVA *(p <* 0.05). *Post hoc* Tukey's multiple comparison test was used to determine the differences between means. For statistical analysis between two groups, a paired Student's *t*-test was performed. Outliers in the data were removed upon the completion of a Grubb's test. The level of significance is indicated by *$p < 0.05$ and was significantly different. At times it is indicated that, **$p < 0.01$, ***$p < 0.001$ and ****$p < 0.0001$. Unless otherwise specified, the error bars were represented by SD.

28

CHAPTER 4 – RESULTS

4.1 PMA activation caused glycogen accumulation in PBMCs

To test my hypothesis, I established protocols to simulate an immune response *in vitro* using standard activating stimuli. The PBMCs were activated with PMA and anti-CD3, and then the cells were observed with light microscopy to confirm their activation. PBMCs have the tendency to cluster together when activated. Using light microscopy, it is possible to observe these PBMC clusters. For the first experiment, PBMCs were incubated for 24 hours in complete media with no stimulus to establish the baseline negative control (Figure 6A). These non-activated PBMCs were dispersed across the bottom of the cell culture plate and formed little to no clustering. PBMCs activated with PMA and anti-CD3 for 24-hours formed clusters after activation, which were indicated by arrows in the image (Figure 6B). For the second experiment, PBMCs were incubated for 24-hours in complete media without stimulus to establish a baseline negative control (Figure 6C). PBMCs activated with soluble anti-CD3 and anti-CD28 antibodies formed clusters (Figure 6D). This data suggests that the PBMCs treated with PMA+anti-CD3 and soluble antibodies (anti-CD3/anti-CD28) were appropriately activated since clustering is a hallmark of T lymphocyte activation.

In the laboratory's previous results, glycogen was shown in PBMC. My first step was to modify the procedure to accommodate more test groups by switching from a slide-based technique to a 96-well plate-based technique. With this modification I could increase the biological replicates and compare more groups. I confirmed that the PAS-staining results could be reproduced with the modified methodology. PBMCs were cultured for 24 and 48-hours with or without PMA+anti-CD3. Subsequently, PBMCs were stained for glycogen using PAS stain. PAS reacts with the glycogen polymer turning it a purple color. According to previous findings, glycogen specifically appears as diffuse signal throughout the cell, and in punctate purple granules. Non-activated PBMCs had no punctate purple granules and low diffuse signals (Figure 7A). In contrast, activated PBMCs had an intense signal and visible punctate granules (Figure 7B). Resolved granules were formed 48-hour after activation with PMA+anti-CD3. An increase in mean signal intensity indicated PAS-glycogen increase. The more glycogen granules there were in the cell, the higher the signal intensity for PAS was. There was a trend to increase in mean signal intensity for PAS-glycogen after 24 and 48-hours compared to non-activated PBMCs (Figure 7C). Lastly, the

PBMCs that were activated with PMA and anti-CD3 for 24 and 48-hours showed a trend to increase in cell area (μm^2), which provided further evidence of their activation since activated cell become larger due to growth and DNA duplication (Figure 7D). This data showed that glycogen accumulated inside the PBMCs following activated with PMA and anti-CD3.
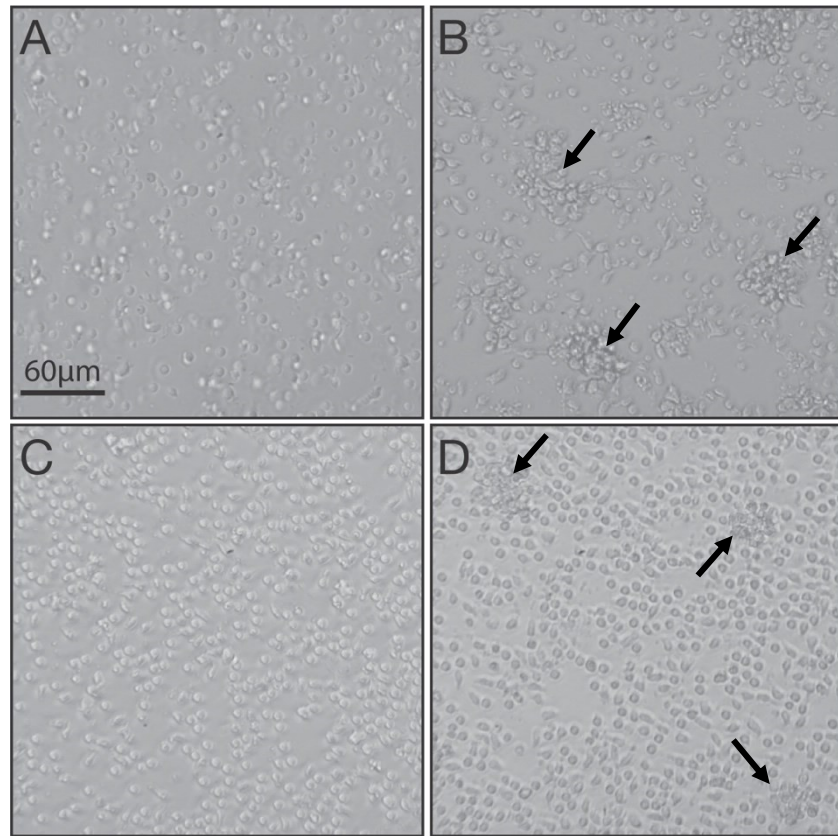
Figure 6 – Evidence that PBMCs were activated at 24-hour time-point

PBMCs were culture for 24-hours with and without activation conditions and then analyzed by light microscopy. The PBMCs were either cultured A) without activation conditions or treated with B) PMA+anti-CD3. PBMCs were either cultured C) without activation conditions or treated with D) soluble antibodies (anti-CD3/anti-CD28). Arrows point to activated cell clusters. Magnification 20x.
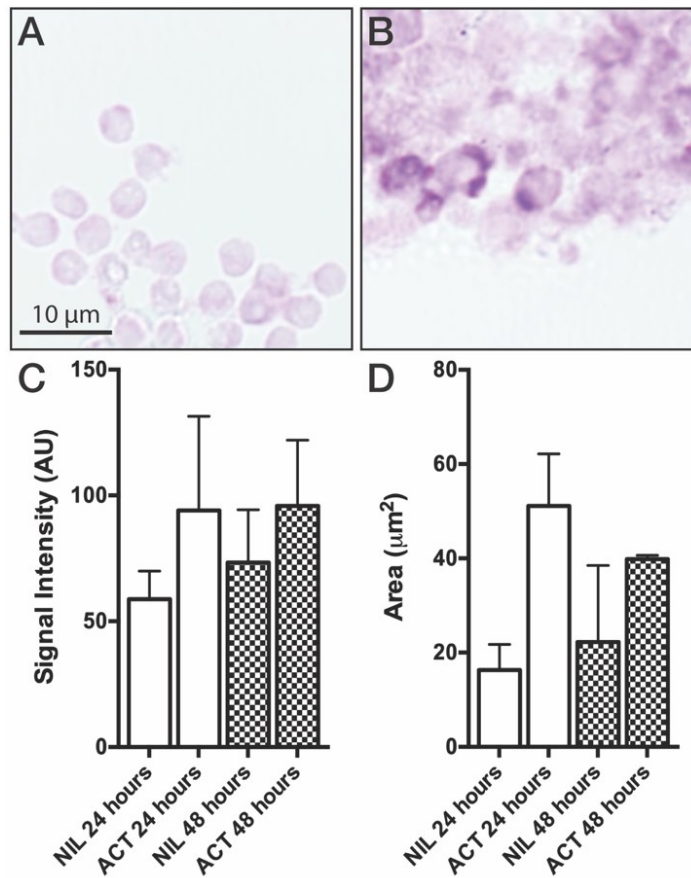
Figure 7 –Evidence of glycogen accumulation in PMA-activated PBMCs

PBMCs were cultured for 24 and 48-hours with PMA plus anti-CD3. PBMCs were cultured **A)** without-activation conditions or with **B)** PMA+anti-CD3. **C)** Signal intensity was recorded using the macro from Appendix 1 (Figure S1) in Fiji software. **D)** PBMC area (μm^2) was calculated from the regions of interest determined by Fiji software (macro). Error bars are representative of the SD between 1 experiment with 5 technical replicates. Magnification = 40x.

4.2 Activation with anti-CD3 and anti-CD28 caused glycogen accumulation in PBMCs

In the previous section, I activated all cells in PBMC suspension with a combination of PMA and anti-CD3. Since PMA is a chemical and directly activates PKC it is not as biologically relevant as using CD28 stimulation, and PMA can activate other cells in the PBMC. Thus, the PMA activation conditions (even in the presence of anti-CD3) did not provide reliable evidence of glycogen dynamics in T lymphocytes. Therefore, I examined how the glycogen dynamics were regulated in T lymphocytes by using soluble anti-CD3 and anti-CD28. PBMCs were activated for 24 and 48-hours. The PBMCs were then collected, and the glycogen was stained using PAS. After glycogen staining, PBMCs were imaged using light microscopy. Punctate purple granules appeared in PBMCs that were cultured for 24-hours with anti-CD3/anti-CD28 whereas control PBMCs had no visible granulation (Figure 8A, B). Punctate purple granules were observed in PBMCs 48-hours after activation (Figure 8C). PBMCs that were not activated, had no granule formation after 48-hours (Figure 8D). The signal intensity of PAS was analyzed. The mean signal intensity of the PAS stain represents the signal from the diffuse staining and the punctate granules of glycogen inside the cell. Activation of PBMCs increased the glycogen signal intensity for both 24 and 48-hour time points compared to the respective non-activated controls (Figure 8E). Activation of PBMCs increased the area of the cells had a trend to increase when they were activated with anti-CD3/anti-CD28 for 24-hour and significantly increased in area after 48-hours (Figure 8F). An increase in cell area is an indicator of cell activation. This data demonstrates that T lymphocytes accumulated glycogen upon activation with anti-CD3/anti-CD28.
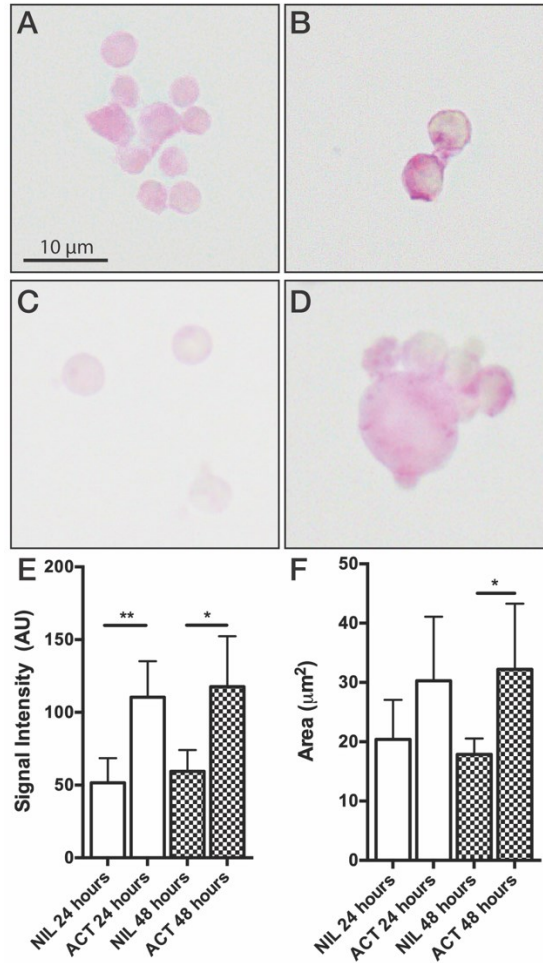
Figure 8 –Evidence of glycogen accumulation in PBMCs activated with soluble antibodies
PBMCs were cultured for 24 and 48-hours with soluble anti-CD3 and anti-CD28. PBMCs were cultured for 24-hours **A)** without soluble antibodies or **B)** with soluble antibodies. PBMCs were in parallel, PBMCs were cultured for 48-hours **C)** without soluble antibodies or **D)** with soluble antibodies. PBMCs were then stained with PAS at the indicated time points **E)** The mean signal intensity for PAS-glycogen was calculated in Fiji (n=5 different participants) at time points of 24 and 48-hours. **F)** Area (μm^2) was measured per condition and time point for each individual (n=5 different participants). Error bars represent SD. Magnification = 40x.

4.3 Isolated Helper CD4$^+$ T cells accumulate glycogen when activated *in vitro*

The focus of this thesis was to investigate glycogen dynamics in purified human helper T cells. The PBMCs tested comprised of a mix of T lymphocytes and other immune cells such as natural killer cells, B cells, monocytes and dendritic cells. The glycogen I detected could have been from the non-T-cells in PBMC suspension. In order to measure glycogen, helper T cells were purified from PBMCs and used for the subsequent experiments. Purified helper T cells were identified by their surface proteins CD4 and CD3 and assessed through flow cytometry.

The flow cytometer provided information on the properties of the cells such as cell size, complexity and protein composition. Based on these properties it is possible to distinguish populations of cells on the 2D histogram output. For example, live cells appear high on side scatter (indicator of cell complexity) because of the complexity within the cell. Dead cells or debris clustered at the origin of the y-axis and x-axis. Live cells represented over 98% of the representative sample which shows a low level of dead cell/debris (Figure 9A). The proportion of these cells that were helper T cells (that express CD4 and CD3 in the upper right quadrant) were over 97% (Figure 9B). When the data was combined from all the experiments I did, the mean live cells obtained were 92.36% +/- 6.5%, while the helper T cells were 96.25% +/- 1.89 (Figure 9C). This data demonstrates that the helper T cells were of a high level of viability and purity.
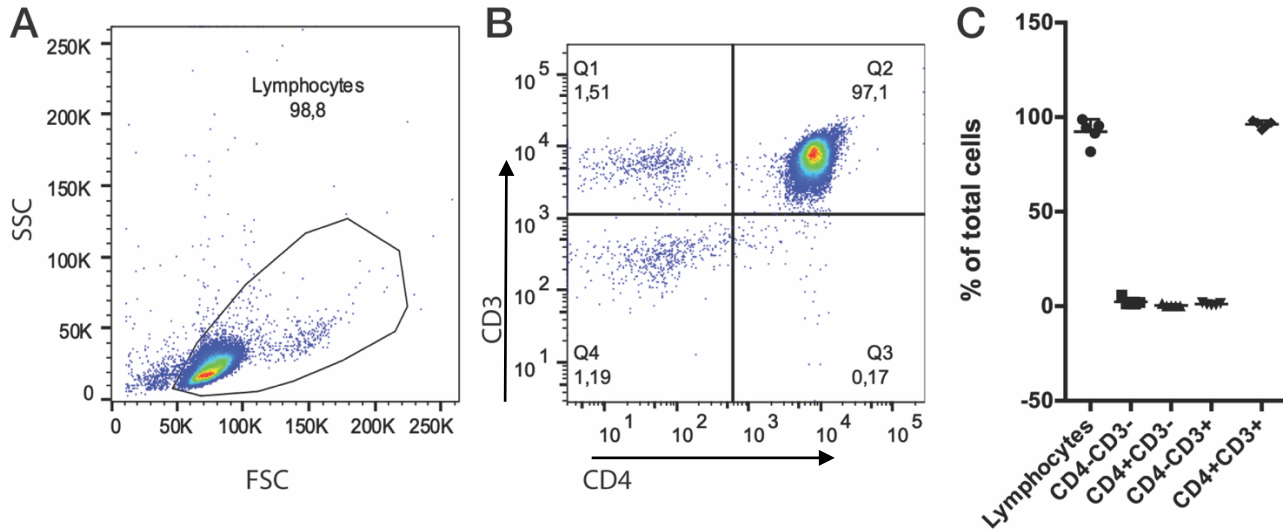
Figure 9 – CD4$^+$CD3$^+$ helper T cell purity confirmation

Helper T cell enrichment was confirmed by flow cytometry. **A)** Live, lymphocyte cells were selected to exclude the dead cells or debris found closer to the intersection of the x-axis and y-axis. **B)** Cells were stained with fluorescent anti-CD3 (APC) and anti-CD4 (PerCP). Gates were established to select the double positive population (Q2) CD4$^+$CD3$^+$. **C)** This represents the percentage of the total amount of cells found to be either lymphocytes or fell into the Q1 (CD4$^-$CD3$^+$), Q2 (CD4$^+$CD3$^+$), Q3 (CD4$^+$CD3$^-$) or Q4 (CD4$^-$CD3$^-$) (n=5 different participants).

Next, glycogen in purified helper T cells was detected using PAS staining. The baseline for PAS-glycogen stain at the 24-hour time point was established using non-activated helper T cells (Figure 10A). Helper T cells that were activated for 24-hours with dynabeads (coated with CD3 and CD28), showed PAS-glycogen granule accumulation (Figure 10B). The baseline for PAS-glycogen at the 48-hour time point was established using non-activated helper T cells (Figure 10C). Helper T cells that were activated for 48-hours showed PAS-stained granules (Figure 10D). The mean signal intensity of PAS-glycogen had a trend to increase after 24-hours of activation with dynabeads (Figure 10E). The mean signal intensity for PAS-glycogen significantly increased in helper T cells activated with dynabeads for 48-hours compared to the non-activated control (Figure 10E). Activated helper T cells significantly increased in cell area when compared to the non-activated control for both 24 and 48-hour time points (Figure 10F). As a negative control, helper T cells were treated with α-amylase prior to PAS-glycogen staining. The α-amylase digested the glycogen prior to staining and therefore was used as a negative control for the PAS histological staining technique. There was no significant difference between the mean signal intensity of activated helper T cells treated with the α-amylase and the non-activated helper T cells (Figure 10G). Non-activated helper T cells and the α-amylase negative control had a significantly lower mean signal intensity to activated helper T cells that were not treated with α-amylase (Figure 10G). This data shows that activation of purified helper T cells results in glycogen accumulation.
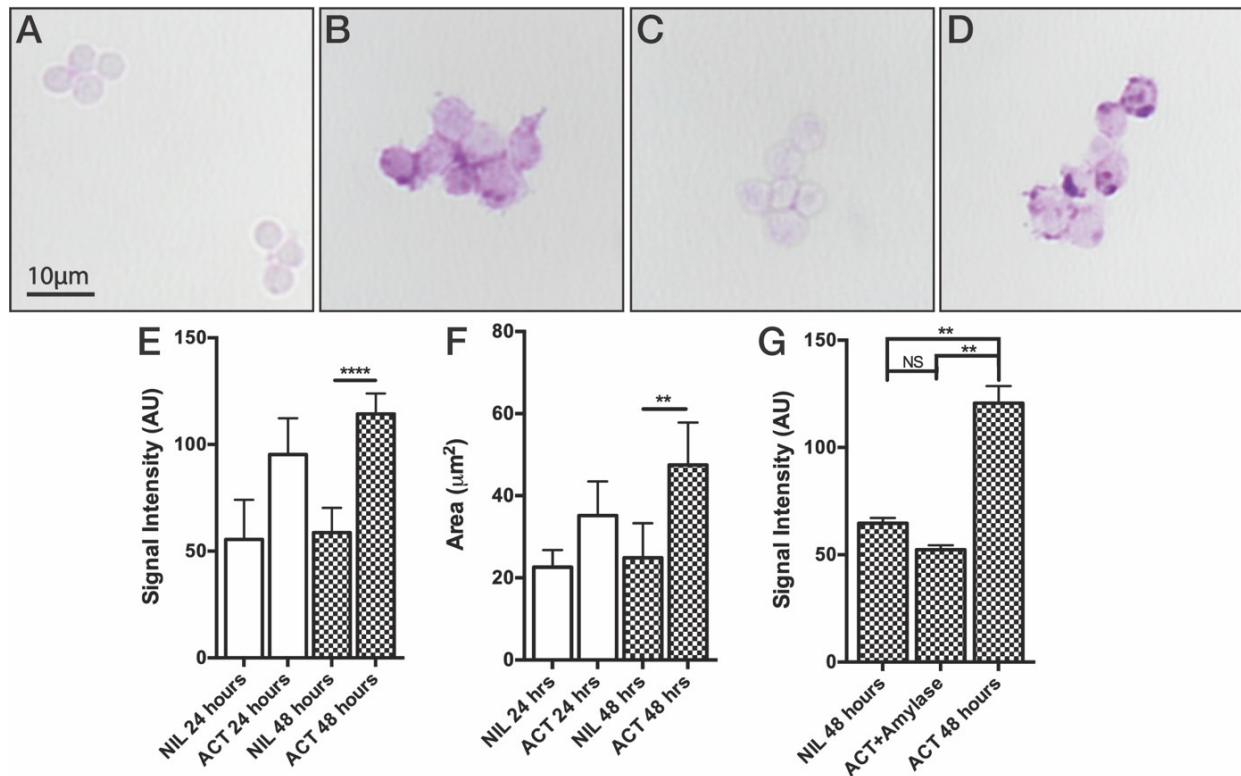
Figure 10 – Helper T cells accumulated glycogen upon activation

Purified helper T cells were cultured for 24 and 48-hours with dynabeads coated with CD3 and CD28, then stained with PAS. Helper T cells were placed in culture **A)** without dynabeads or **B)** with dynabeads for 24-hours. In parallel, helper T cells were placed in culture **C)** without dynabeads or **D)** with dynabeads for 48-hours. The mean PAS-glycogen signal intensity was calculated using Fiji software (n=5 different participants) at time points of **E)** 24 and 48-hours. **F)** The cell area (μm^2) was measured per condition and time point of each individual (n=5 different participants). **G)** After being cultured for 48-hours, helper T cells were treated with α-amylase in order to digest glycogen prior to staining as the negative control (data pooled from 2 participants done in duplicates). Magnification = 40x

4.4 Glycogen breakdown inhibition alters the proliferation profile of PBMCs *in vitro*

The function of glycogen storage in helper T cell is not well known. The highly proliferative property of T lymphocytes is one of their defining features. Therefore, it was important to explore the way glycogen metabolism could affect proliferation. PBMCs were activated with T lymphocyte specific activators (anti-CD3 and anti-CD28) with or without GPI. GPI works as a potent competitive inhibitor for glycogen phosphorylase and has been shown to inhibit glucagon induced glycogenolysis in hepatocytes *in vitro* (Klabunde *et al.,* 2005). The effects of GPI on proliferation and cytokine production were measured. It can be speculated that GPI inhibited glycogenolysis and therefore resulted in the inhibition of glycogen-derived glucose supply to the cell. Non-activated PBMCs were used to establish a baseline control for PAS-glycogen staining (Figure 11A). PBMCs accumulated PAS-glycogen granules when activated with or without GPI (Figure 11, B and C). Mean signal intensity for PAS-glycogen increased by approximately 2-fold in activated PBMCs treated with GPI compared to the non-activated control (Figure 11D). To measure the effect of GPI on proliferation, PBMCs were activated in the presence of GPI for 4 days in media with 1% serum. The PBMCs were treated with CFDA-SE to monitor proliferation (explained further in section 3.6). PBMCs, activated in the presence of GPI proliferated 10% less ($p < 0.01$) than PBMCs activated without GPI (Figure 11E). Activated PBMCs with GPI proliferated almost 20% more than non-activated PBMCs (Figure 11E). GPI affected the production of pro-inflammatory cytokine IL-17A. Activated PBMCs that were treated with GPI had a trend to decrease in IL-17A production when compared to activated cells without GPI treatment (Figure 11F). This data suggests that glycogenolysis may play a role in proliferation and cytokine production of helper T cells.
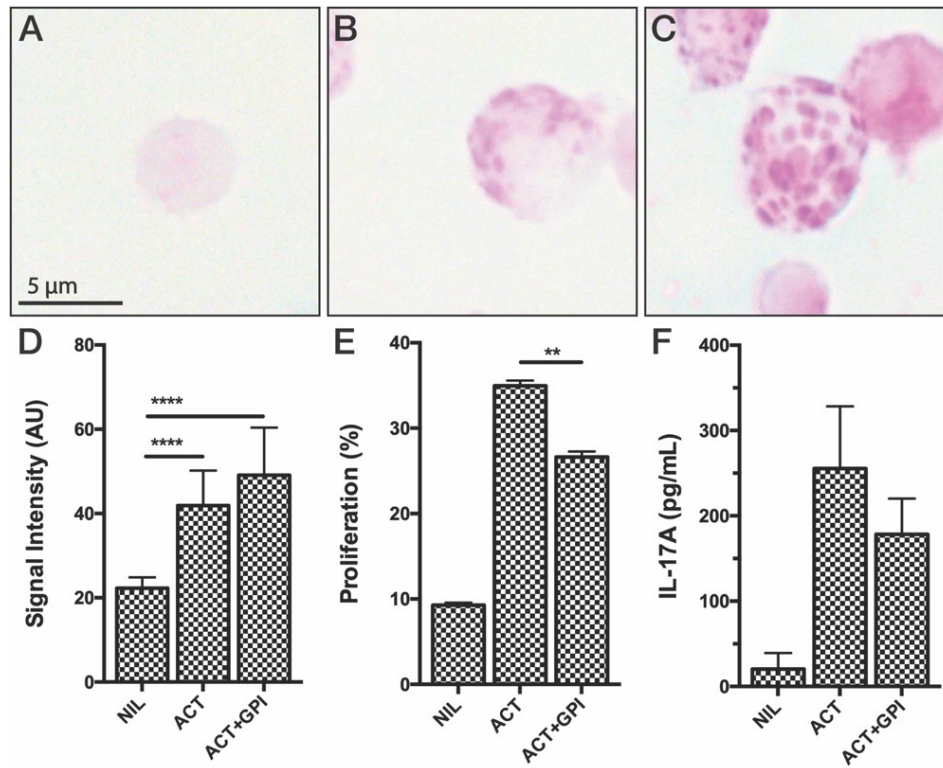
Figure 11 –Effect of GPI on glycogen accumulation and proliferation in activated PBMCs
PBMCs were either **A)** not activated, **B)** activated with soluble antibodies or **C)** activated with soluble antibodies with the addition of GPI. PBMCs were then stained for glycogen using PAS. **D)** The mean signal intensity for PAS-glycogen was analyzed with Fiji software. **E)** Proliferation was assessed using CFDA-SE and was analyzed via Flow cytometry. **F)** IL-17A concentration in the supernatant was measured via ELISA. For this experiment. PBMCs were grown in RPMI with 1% serum. Magnification = 60x

4.6 2-NBDG is useful in human astrocytes but not in lymphocytes to detect glycogen

Besides for PAS histological stain, there are very few established methods for visualizing glycogen in helper T cells. 2-NBDG is a fluorescent analog of glucose that is primarily used to record glucose uptake. I wanted to test whether 2-NBDG could incorporate itself into the glycogen polymer in the helper T cells and therefore provide a more versatile means to visualize glycogen than PAS. To test this method, human astrocytes were used as a control. There is literature showing that glycogen is important for astrocyte cell function. 24-hours prior to manipulation, astrocytes were made reactive by adding IL-1β cytokine. Reactive astrocytes take up glucose at a higher rate than non-reactive astrocytes (Chen *et al.,* 2015b). Both reactive and non-reactive astrocytes took up 2-NBDG. In resting astrocytes, fluorescence was dispersed throughout the cytoplasm (Figure 12, left panels). Reactive astrocytes had punctate granules of 2-NBDG (Figure 12, right panels). The punctate granules seen in the cytoplasm of the astrocytes are most likely glycogen molecules. The conclusions are two-fold; 2-NBDG can detect glycogen in astrocytes, and astrocytes accumulate glycogen when made reactive with pro-inflammatory cytokine IL-1β.

Since 2-NBDG was incorporated into glycogen in reactive astrocytes, the next steps were to translate this method to helper T cells. Before using primary T lymphocytes, Jurkat T cells were used as a control. Jurkat T cells are an immortalized T lymphocyte cell line commonly used for *in vitro* experimentation. These cells are simple to culture and proliferate highly when activated. Jurkat T cells were cultured with 2-NBDG in activation conditions for 24 and 48-hours. Activated Jurkat T cells seemed to have taken up 2-NBDG and formed granules (Figure 13 right panels). However, activated Jurkat T cells, in the absence of 2-NBDG, had high background fluorescence in the green channel (Figure 13 middle panels). A similar signal was observed in non-activated Jurkat T cells (Figure 13 left panels). This indicated that Jurkat T cells either are auto-fluorescent for this wavelength or that Jurkat T cells were not taking up 2-NBDG as efficiently as foetal astrocytes. PBMCs were also treated with 2-NBDG and the same results were observed (Figure S3).
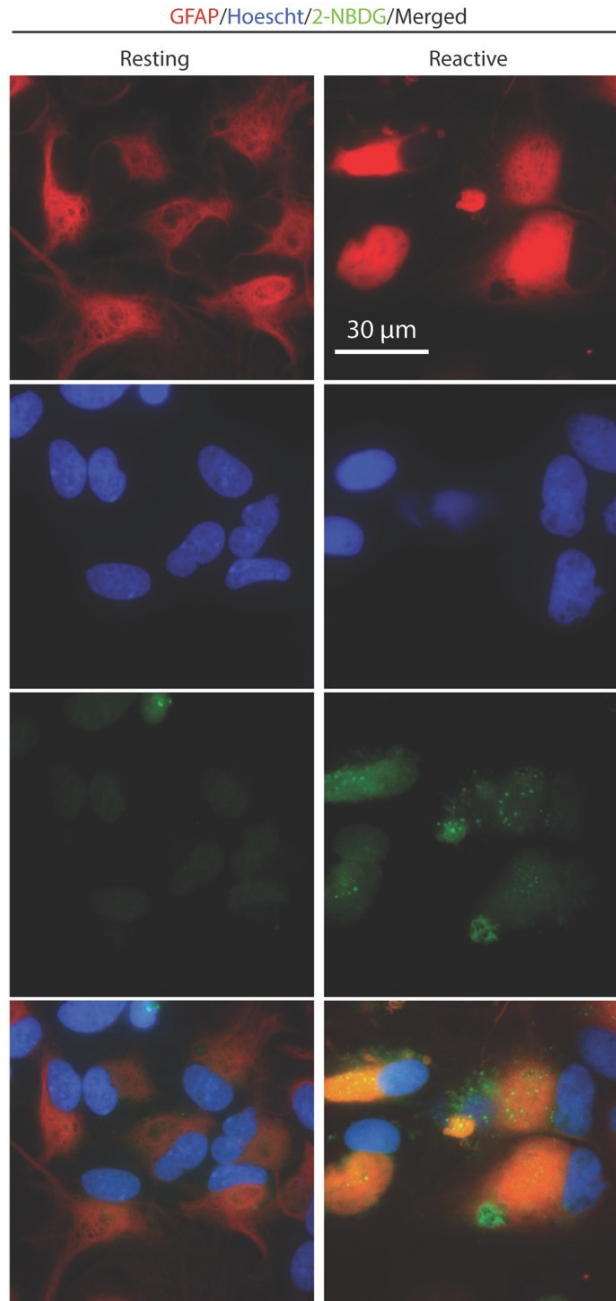
Figure 12 – 2-NBDG is incorporated into glycogen in reactive human astrocytes

Immunofluorescent images of foetal human astrocytes show 2-NBDG (green) accumulation and granule formation inside the cells. GFAP (red), an intermediate filament only in astrocytes, shows the cell shape. Overlap between 2-NBDG granules and GFAP would indicate the granules are located inside the cell. Hoechst (blue) was used as a nuclear stain. Scale bar = 30 μm.
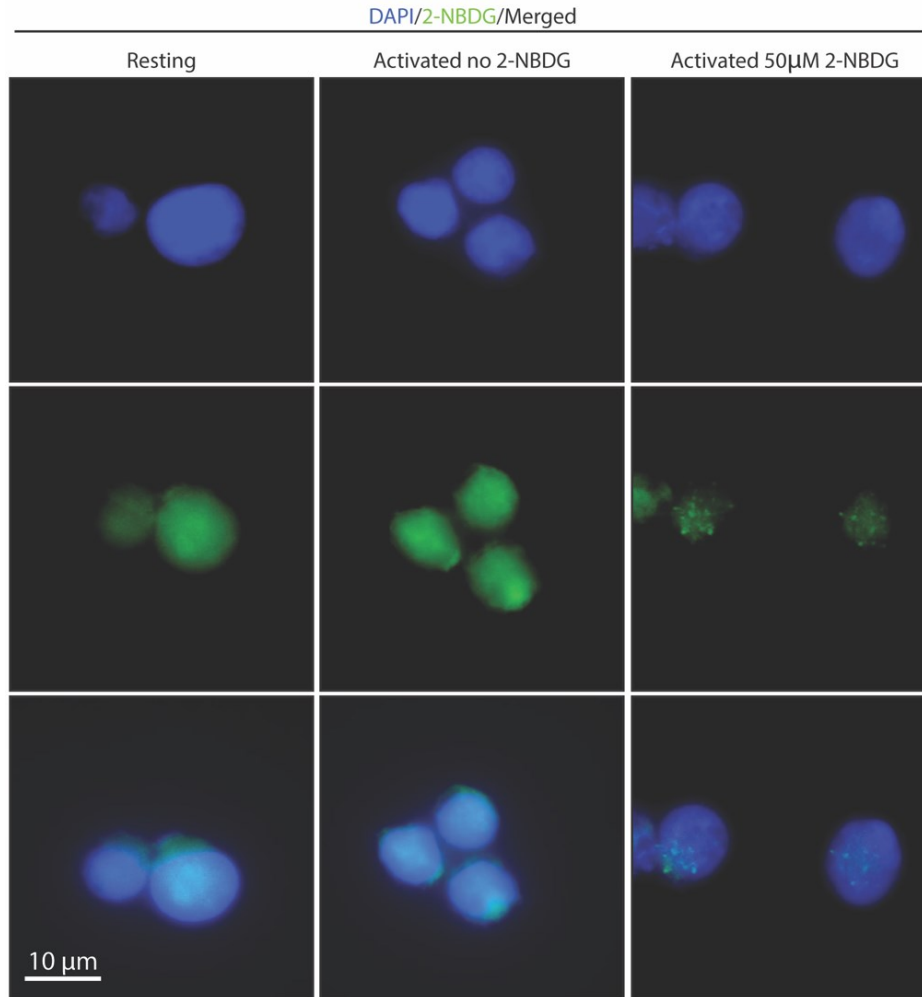
Figure 13 – 2-NBDG in Jurkat T cells

Immunofluorescent images of Jurkat T cells show 2-NBDG (green) accumulating and forming granules inside the cells during activation. However, Jurkat T cells are auto-fluorescent and therefore 2-NBDG is currently an unreliable method for measuring glycogen in helper T cells. 2-NBDG signal (green) is observed in control conditions (no 2-NBDG). DAPI (blue) was used as a nuclear stain. Magnification = 60x

This data suggests that 2-NBDG was not yet suitable to measure glycogen in Jurkat T cells and PBMCs (Figure S3). More optimization is required for 2-NBDG to become an efficient method for glycogen measurement in T lymphocytes.

4.5 RNA expression for genes involved in glycogen dynamics in helper T cells

My results indicated that glycogen was important for T lymphocyte metabolism. I sought to determine to what extent glycogen genes were being differentially expressed during helper T cell activation. NIH's Genome Expression Omnibus (GEO) is a public repository for genomic data submissions. I compiled data from two data sets (Gate *et al.,* 2018; Komori *et al.,* 2015). RNAseq data was aligned and processed by the authors and was made public in a ready to read file format. Experimental set-up was similar for both data sets. However, the two data sets were not comparable due to the formulas used to report the results (RPKM vs. TPM). From the data sets I compared the expression of genes involved in the glycogen pathway. Gene expressions from activated helper T cells with dynabeads were compared to non-activated helper T cells. RNA expression varied in activated naïve helper T cells for 48-hours compared to non-activated helper T cells. For the Komori *et al.,* 2015 data set, glycogen synthase isotypes (*GYS1* and *GYS2*) increased by ~2-fold when helper T cells were activated for 48-hours (Figure 14A). Brain glycogen phosphorylase (*PYGB*) increased in activated helper T cells while liver and muscle glycogen phosphorylase (*PYGL* and *PYGM*) decreased in expression when activated (Figure 14B). Phosphoglucomutase (*PGM1* and *PGM2*) expression increased by ~4-fold and ~2-fold, respectively (Figure 14C). In helper T cells, UDP-glucose pyrophosphorylase 2 (*UGP2*), glycogenin (*GYG1*) and glucose channel 1 (*SLC2A1*) increased by ~1.5-fold, ~0.2-fold and ~0.7-fold respectively when activated (Figure 14D). For the Gate *et al.,* 2018 data set, *GYS1* gene increased in expression by ~2-fold when helper T cells were activated (Figure 15A). *GYS2* showed no change in expression (Figure 15A). *PYGB* increased in activated helper T cells by ~1-fold while the expression of *PYGL* and *PYGM* decreased or remained mostly unchanged when activated (Figure 15B). *PGM1* and *PGM2* expression increased by ~2-fold and ~4-fold respectively (Figure 15C). In helper T cells, *UGP2*, *GYG1* and *SLC2A1* increased by <1-fold, <1-fold and ~4-fold respectively when activated (Figure 15D). These data sets provided evidence to the difference in expression of proteins involved in key glycogen pathways in helper T cells.

Figure 14 – Gene expression for transcripts involved in glycogen dynamics (derived from Komori *et al.*, 2015)

RNAseq data was modified from Komori *et al.,* 2015 obtained from the GEO public database. RNAseq data was represented as RPKM. The formula to determine RPKM can be found in Appendix 1 formula 2. The fold-change between non-activated and activated helper T cells was calculated. **A)** Change of mRNA expression for two isoforms of glycogen synthase (*GYS1* and *GYS2*). **B)** Change of mRNA expression for three isoforms of glycogen phosphorylase; brain, liver and muscle (*PYGB*, *PYGL* and *PYGM*). **C)** Change of mRNA expression for two isoforms of phosphoglucomutase (*PGM1* and *PGM2*). **D)** Change of mRNA expression for three proteins involved in glycogen dynamics: UDP-glucose pyrophosphorylase 2, glycogenin 1 and glucose transporter 1 (*UGP2*, *GYG1* and *SLC2A1*). Error bars represent the standard error of the mean (SEM). Raw data can be found using GEO accession number GSE59860.
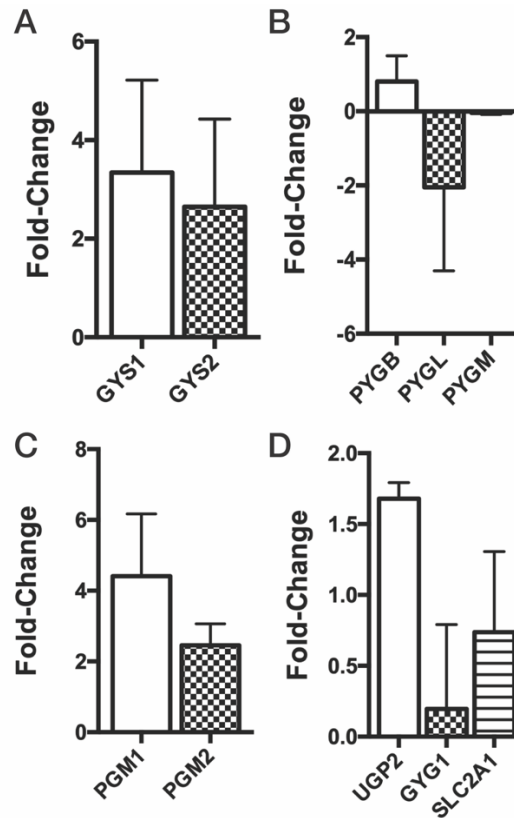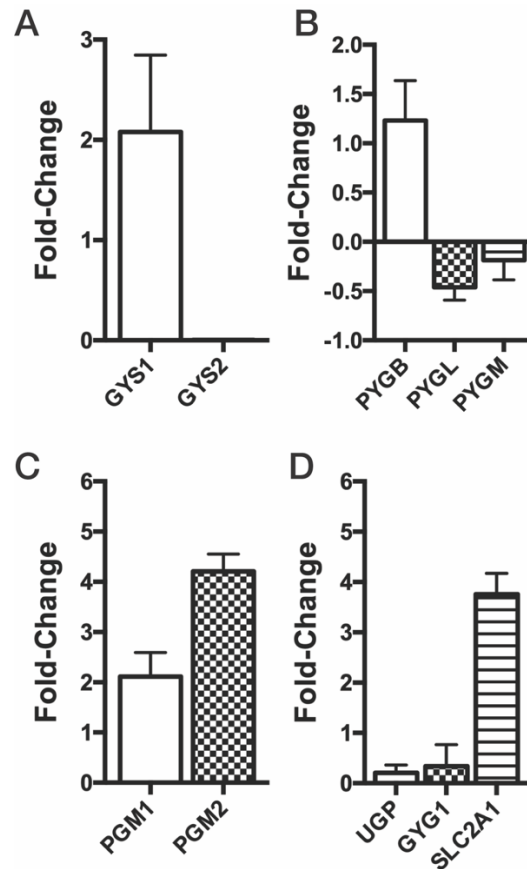
Figure 15 - Gene expression for transcripts involved in glycogen dynamics (derived from Gate *et al.*, 2018)

RNAseq data was modified from Gate *et al.,* 2018 obtained from the GEO database from. RNAseq data was represented as TPM. The formula to determine TPM can be found in Appendix 1 formula 3. The fold-change between non-activated and activated helper T cells was calculated. **A)** Change of mRNA expression for two isoforms of glycogen synthase (*GYS1* and *GYS2*). **B)** Change of mRNA expression for three isoforms of glycogen phosphorylase; brain, liver and muscle (*PYGB*, *PYGL* and *PYGM*). **C)** Change of mRNA expression for two isoforms of phosphoglucomutase (*PGM1* and *PGM2*). **D)** Change of mRNA expression for three proteins involved in glycogen dynamics: UDP-glucose pyrophosphorylase 2, glycogenin 1 and glucose transporter 1 (*UGP2*, *GYG1* and *SLC2A1*). Error bars represent SEM. Raw data can be found using GEO accession number GSE86888.

CHAPTER 5 – DISCUSSION

The purpose of this thesis was to investigate the dynamics of glycogen in purified helper T cells. The first aim was to observe glycogen accumulation in activated helper T cells. The second aim was to assess the effects of glycogenolysis inhibition on T lymphocyte proliferation and cytokine production. The third aim was to investigate the change in expression of genes involved in glycogen dynamics in activated helper T cells. This is one of the first times glycogen dynamics in helper T cells was studied, while successfully demonstrating its presence and significance to effector function.

5.1 Glycogen dynamics in PBMCs

The study of glycogen dynamics in activated PBMCs sheds light on the larger role glycogen plays in an immune response. PBMCs were stimulated *in vitro* with either small molecule PMA or soluble antibodies. It is speculated that PMA directly acted upon PKC and therefore activated all cell types in suspension, where the soluble antibodies provided the necessary signals for activation of the T lymphocytes within PBMC suspensions. Activated PBMCs, that were stained with PAS, had purple glycogen granules dispersed throughout the cytoplasm. An increase in mean signal intensity of the PAS stain within the PBMCs confirmed that glycogen stores had increased due to activation, which supports previous findings. Although there was an overall increase in PAS-glycogen, not all activated PBMCs contained granules. There was no consistent pattern to determine which cells contained granules (location of granules within the cell or size and morphology of the cells). Some PBMCs showed purple punctate granulation patterns while others had diffused purple staining (Figure S2). This sporadic staining trend is consistent with previous literature (Tabatabaei Shafiei, 2016).

The cells that had PAS-glycogen did not always have punctate granules; certain cells also had diffuse staining. The reason for differences in staining patterns for PAS-glycogen is still unclear. 24-hours after activation, the staining was prominently diffuse, whereas after 48-hours there appeared to be more resolved punctate granules. Not all of the activated cells had glycogen granules (either diffuse or granulated). A lack of glycogen accumulation in some cells could be due to several factors. While naïve T cells made up the majority of T lymphocytes in the extracted

blood, there is a fraction of differentiated helper T cells (Th1, Th2, Th17, Th9, Th22 and Treg), cytotoxic T cells and memory T cells that could be present in suspension (Kleiveland, 2015). Activation of PBMCs with anti-CD3/anti-CD28 would have resulted in the activation of a heterogeneous population of T lymphocytes. Each T lymphocyte subset could have a varied use for glycogen. Differentiated T lymphocytes are identified by their surface proteins and expression of different cytokines. It is possible that differentiated T lymphocytes use glycogen for different reasons depending on their cell type and life stage at the time of activation. As an example, there could have been cytotoxic T cells present in the suspension. There is evidence that glycogen plays a role in the ability for CD8 cytotoxic T cells to differentiate into memory cells (Ma *et al.,* 2018).

Isolated PBMCs contained a high ratio of T lymphocytes but were also composed of B lymphocytes, natural killer cells, monocytes and a small percentage of DCs. Prior knowledge of glycogen dynamics exists for DCs, and cytotoxic T cells, meaning the glycogen accumulation could very well be coming from cells that are not T lymphocytes. Monocytes could be stimulated by IL-17A and may be an explanation for the larger cells captured in figure 8D that contained glycogen granules (Erbel *et al.,* 2014). The anti-CD3/CD28 activation provided validation to the altered PAS-staining technique and therefore endorsed the testing of glycogen dynamics on isolated helper T cells.

5.2 Glycogen dynamics in activated helper T cells

The use of purified populations of helper T cells was important to reduce unwanted discrepancies coming from a mixed population of cells. Isolated helper T cells accumulated glycogen when activated *in vitro*. There were differences in glycogen granule morphology throughout the time course as well. At the 24-hour time point, a few helper T cells had observable glycogen granulation despite the evidence of activation. After 48-hours, the proportion of helper T cells containing substantial granulation appeared to increase from 24-hour activated helper T cells. The non-activated control was used as a baseline because there were no PAS-granules. The stain became concentrated in the granules instead of being diffused throughout the cytoplasm. Glycogen granules appeared larger, more resolved and abundant at 48-hours. The significant increase in PAS-glycogen signal intensity validates the aforementioned observation. Previously, Tabatabaei Shafiei observed, in activated PBMCs, that the smaller cells (which were most likely lymphocytes, defined by a diameter of $< 5\mu$m), were almost all positive for glycogen. Using

isolated helper T cells, there was an observable proportion of overall glycogen positive cells than was seen in PBMCs. This supported previous findings that glycogen granules are primarily found in T lymphocytes within PBMC suspensions. Furthermore, of the observed stained helper T cells, some cells contained glycogen granulation. Therefore, the question still remained; which are the cells that contain glycogen?

Not all activated helper T cells visibly contained glycogen granules *in vitro*. Since a heterogenous population of helper T cells was activated *in vitro,* the next step would be to determine which cell type accumulated glycogen in the initial stages of activation. This thesis presents novel evidence that glycogen accumulation peaks at 48-hours post activation with anti-CD3/anti-CD28 in both PBMCs and isolated helper T cells. In most cases, a naïve helper T cell response *in vivo* peaks between 7-15 days after being exposed to its cognate antigen (Pennock *et al.,* 2013). Memory helper T cells are primed and significantly quicker at responding to stimulus (proliferating and producing cytokines) than naïve helper T cells. In the blood of our participants, and therefore in the isolated helper T cells used for our experimentation, a small percentage of cells were most likely effector memory helper T cells or other already differentiated helper T cell subsets (Th1, Th2, Th17, etc.). Future directions would involve sorting the helper T cells into subsets to better understand how glycogen dynamics vary between differentiated helper T cells. Single-cell RNAseq could be used in tandem to analyze RNA expression of glycogen pathway genes in differentiated helper T cells.

5.3 Glycogenolysis inhibition and T lymphocyte proliferation

Inhibition of glycogenolysis in PBMCs resulted in the reduction of proliferation and pro-inflammatory cytokine production. I showed that inhibition of glycogen breakdown in activated T lymphocytes caused a greater accumulation of glycogen than PBMCs activated alone. Additionally, treatment with GPI resulted in a significant decrease in proliferation for PBMCs *in vitro.* GPI has limitations because it can have off-target effects on the T lymphocytes that could be influencing their effector function. Although the concentration of inhibitor used was in accordance with the manufacturer's instructions it would be useful, in the future, to assess the proper GPI concentration using a dose response.

Glycogen dynamics varied depending on the serum levels. Glycogen signal intensity was lower for PBMCs cultured in 1% serum than those cultured in 10% serum. This reflected the

findings from Tabatabaei Shafiei 2016, where she found, using a serum titration experiment, that glycogen availability in PBMCs was dependent on there being higher serum levels during activation with anti-CD3/anti-CD28 *in vitro*. In culture, glucose availability is primarily dependent on the amount of serum (FBS was used in this thesis) added to media preparations. It is possible that, in a low glucose environment (simulated using media with 1% serum), activated PBMCs quickly depleted glycogen to ensure they could continue to proliferate. Therefore, glycogen could be used to ensure the cell has a sufficient supply of glucose to continue carrying out its effector functions.

5.4 Glycogen pathway mRNA expression in activated helper T cells

In activated helper T cells, there was a difference in the expression of genes involved in glycogen pathways. Two publicly available GEO data sets were analyzed individually to make inferences about the RNA expression. The authors published data using two different formulas to obtain their data; TPM and RPKM (Appendix 1, formula 2 and 3). In both cases, the transcript profile changed for important glycogen related genes in response to 48-hours of activation with dynabeads. In helper T cells, there was a change in expression for genes involved in both glycogenesis and glycogenolysis due to activated. Helper T cells could favor the breakdown or synthesis of glycogen depending on the need at the time in the cell cycle. Glycogen could be degraded to provide biosynthetic substrate in preparation for G1/S phase. Alternatively, the cell could favor glycogen accumulation when the cell does not require as many by-products derived from glycolysis. While this RNAseq data provides insight into the change in expression for genes involved in glycogen dynamics, there could also be changes at the protein level. Post-translational modifications of proteins could be responsible for changes in the glycogen dynamics profile, of the helper T cells, to favour either glycogenesis or glycogenolysis. This RNAseq data could be coupled with future protein analysis such as mass spectroscopy followed by enzyme assays to determine the changes in activity of certain enzymes involved. This data provided evidence that in helper T cells glycogen can be broken down at the same time as it can be rebuilt, and cements the idea that glycogen is a dynamic polymer used by helper T cells.

5.5 Role of glycogen in helper T cells

There has been limited work done on glycogen dynamics in helper T cells. It was important to obtain information from other cell types to make valid speculations, because of the lack of prior literature on glycogen dynamics in helper T cells. In this thesis, I used astrocytes as a control to optimize and establish 2-NBDG, in order to eventually observe glycogen in lymphocytes. The literature on glycogen dynamics in astrocytes is useful in order to draw inferences on how glycogen dynamics occurs in helper T cells. One job of an astrocyte is to metabolize glycogen into lactate and then shuttle it to neurons. Similarly, helper T cells provide a support role in immunity. Like astrocytes, activated helper T cells produce an increased amount of lactate in an inflammatory environment (Grist *et al.,* 2018). Lactate production, from helper T cells, could be used to modulate the activity of other immune cells in the inflammatory microenvironment. Immune cell modulation, due to lactate, has been studied in a tumor microenvironment where cytotoxic T cells take up lactate, leading to their inhibition (Fischer *et al.,* 2007). Glycogen accumulation in helper T cells could be a way for them to provide signalling to other immune cells in response to a stimulus. There are possibly other physiological functions to glycogen in activated helper T cells.

Glycogen could be important for regulating osmotic pressure when the helper T cell proliferates. Activated helper T cells need to acquire glucose during an immune response. The increase in soluble glucose disrupts the osmotic pressure of the cell. Glycogen does not cause an osmotic imbalance for the cell, and therefore, could be a method for them to effectively store surplus glucose. Glycogen accumulation may allow the helper T cell to modulate the function of other immune cells while ensuring they do not encounter a disproportion of osmotic pressure.

5.6 Future directions

One direction of this project could be to improve upon the techniques for glycogen visualization, in order to better track the dynamics of glycogen in helper T cells. The current limitation of PAS-glycogen signal intensity measurements is that small changes in concentration are difficult to record. Expansion of glycogen visualization techniques with 2-NBDG would allow for higher resolution images of glycogen and therefore a better representation of small changes in glycogen concentration. Additionally, 2-NBDG could provide an optimal tool for visualizing glycogen dynamics in real time. 2-NBDG also would be a useful technique to explore earlier time points of activation. I explored glycogen dynamics at 30-minutes, 24, 48 and 72-hours after

activation. There is a possibility that glycogen is most active at earlier time points, which 2-NBDG visualization at earlier time points could address. In the case of helper T cells 2-NBDG can be coupled with fluorescent antibodies to identify specific subsets of helper T cells. For example, using 2-NBDG with fluorescent antibodies for CD4, CD3 and intracellular FoxP3 would allow monitoring of glycogen dynamics in the Treg subset. In addition to 2-NBDG optimization, it would also be useful to obtain a more expansive RNA expression profile for helper T cells, by using single-cell RNA sequencing. With this sequencing data, scientists could more precisely pinpoint which branching glycolytic pathways are required for helper T cell to proliferate and undergo clonal expansion. These proposed experiments would provide more evidence that glycogen is accumulating in helper T cells.

Future directions should address the functionality of glycogen in the helper T cell. Further analysis using inhibitors for the glycogen pathway (for both glycogenesis and glycogenolysis) would be useful in establishing the role of glycogen in activated helper T cells. Here, it was shown that GPI had a negative effect on the proliferation of helper T cells *in vitro*. It would be useful to find other gene targets that could either be knocked out or inhibited without affecting other important processes within the cell. Adoptive transfer of helper T cells post immunoablation, in a diseased/infection animal model (mice for example) would provide a newfound understanding of how glycogen dynamics in helper T cells affects the immune systems' ability to fight infection or disease *in vivo*.

5.7 Studying glycogen metabolism in helper T cells to understand health and disease

In the 1960s, there were reports that the activation of PBMCs caused glycogen accumulation. The changes in glycogen concentration was being explored as a diagnostic tool for cancers. In patients with chronic or acute lymphocytic leukemia, lymphocytes had increased glycogen levels (Bennett and Dutcher, 1969). The Quaglino and Hedeskov group attempted to use PAS staining to create a link between increases in glycogen content in lymphocytes and cancer diagnosis (Hayhoe and Quaglino, 1965; Hedeskov, 1968). Controversial findings contributed to the abandonment of PAS staining as a diagnostic tool for cancer (Jones *et al.,* 1962; Leder and Donhuijsen, 1978). PAS-positivity was an indication of prognosis only for cancers effecting lymphocytes directly, such as lymphoblastic leukemia and Hodgkin's disease. Even though PAS

staining was not a good diagnosis for all cancers, PAS-glycogen staining in lymphocytes was integrated into the diagnosis of a lysosomal disorder called Pompe's disease.

In the lymphocytes of patients with glycogen storage disease (GSD), such as Pompe's disease, their lysosomes fail to degrade glycogen and accumulate autophagic vacuoles that stain purple with PAS (Hagemans *et al.,* 2010; Pascarella *et al.,* 2018). PAS test can be done on blood smears, making it a fast and easy test. For GSD, enzyme replacement therapy is most common. Specifically, mutations in acid alpha-glucosidase gene (*GAA*) are responsible for the enzymes inability to cleave glycosidic bonds of glycogen in lysosomes. Since its introduction in 2006, restoration of glycogen dynamics through gene therapy has reduced instances of mortality and morbidity of GSD (Pascarella *et al.,* 2018). This highlights a prime example of glycogen dynamics in lymphocytes playing an important role in health and disease.

5.8 Conclusion

To summarize, I provided evidence of glycogen accumulation in helper T cells. Based on the results, there is reason to believe that glycogen dynamics play a role in the effector function of helper T cells. This is amongst the first accounts of glycogen dynamics in helper T cells. Helper T cells are one of the most important cells of the immune system. The presence of glycogen dynamics in helper T cells and its involvement in proliferation could reveal its usefulness as a target for therapy with future experimentation. There is still a lot to be learned about helper T cells and their metabolism. It is important to continually uncover new pathways that affect their function. The more knowledge that becomes available on healthy immune cells, the better chance there is to uncover abnormalities that lead to diseases.

BIBLIOGRAPHY

Aderem, A., and Ulevitch, R.J. (2000). Toll-like receptors in the induction of the innate immune response. Nature *406*, 782–787.

Alberts, B., Johnson, A., and Lewis, J. (2002). Introduction to Pathogens. In Molecular Biology of the Cell, (New York: Garland Science), pp. 1485–1501.

Alberts, B., Bray, D., Hopkins, K., Johnson, A., Lewis, J., Raff, M., and Roberts, K. (2009). In Essential Cell Biology, (Garland Science), pp. 426–450.

Antel, J.P., Lin, Y.H., Cui, Q.-L., Pernin, F., Kennedy, T.E., Ludwin, S.K., and Healy, L.M. (2018). Immunology of oligodendrocyte precursor cells in vivo and in vitro. J. Neuroimmunol. *331*, 28–35.

Appleman, L.J., Berezovskaya, A., Grass, I., and Boussiotis, V.A. (2000). CD28 Costimulation Mediates T Cell Expansion Via IL-2-Independent and IL-2-Dependent Regulation of Cell Cycle Progression. J. Immunol. *164*, 144–151.

Araque, A., Carmignoto, G., Haydon, P.G., Oliet, S.H.R., Robitaille, R., and Volterra, A. (2014). Gliotransmitters travel in time and space. Neuron *81*, 728–739.

Arrizabalaga, O., Lacerda, H.M., Zubiaga, A.M., and Zugaza, J.L. (2012). Rac1 Protein Regulates Glycogen Phosphorylase Activation and Controls Interleukin (IL)-2-dependent T Cell Proliferation. J. Biol. Chem. *287*, 11878–11890.

Artyomov, M.N., Lis, M., Devadas, S., Davis, M.M., and Chakraborty, A.K. (2010). CD4 and CD8 binding to MHC molecules primarily acts to enhance Lck delivery. Proc. Natl. Acad. Sci. U. S. A. *107*, 16916–16921.

Baaten, B.J.G., Li, C.-R., Deiro, M.F., Lin, M.M., Linton, P.J., and Bradley, L.M. (2010). CD44 Regulates Survival and Memory Development in Th1 Cells. Immunity *32*, 104–115.

Bennett, J.M., and Dutcher, T.F. (1969). The Cytochemistry of Acute Leukemia: Observations on Glycogen and Neutral Fat in Bone Marrow Aspirates. Blood *33*, 341–347.

Bental, M., and Deutsch, C. (1993). Metabolic changes in activated T cells: an NMR study of human peripheral blood lymphocytes. Magn. Reson. Med. *29*, 317–326.

Berg, J.M., Stryer, L., Tymoczko, J.L., and Gatto, G. (2010). In Biochemistry, (WH Freeman), pp. 328–329, 615–635.

Bluestone, J.A. (1995). New perspectives of C1328-137-mediated T cell costimulation - ScienceDirect. Immunity *2*, 555–559.

von Boehmer, H. (1992). T cell development and selection in the thymus. Bone Marrow Transplant. *9 Suppl 1*, 46–48.

Brown, A.M., Tekkök, S.B., and Ransom, B.R. (2003). Glycogen regulation and functional role in mouse white matter. J. Physiol. *549*, 501–512.

Carroll, N., Longley, R., and Roe, J. (1956). The Determination of Glycogen in Liver and Muscle by use of Anthrone Reagent. J. Biol. Chem. 583–593.

Chen, R.J., Zhang, G., Garfield, S.H., Shi, Y.-J., Chen, K.G., Robey, P.G., and Leapman, R.D. (2015a). Variations in Glycogen Synthesis in Human Pluripotent Stem Cells with Altered Pluripotent States. PLOS ONE *10*, e0142554.

Chen, Y., Zhang, J., and Zhang, X. (2015b). 2-NBDG as a Marker for Detecting Glucose Uptake in Reactive Astrocytes Exposed to Oxygen-Glucose Deprivation In Vitro. J. Mol. Neurosci. *55*, 126–130.

Cibrián, D., and Sánchez-Madrid, F. (2017). CD69: from activation marker to metabolic gatekeeper. Eur. J. Immunol. *47*, 946–953.

Courtney, P.A., Crockard, A.D., Williamson, K., Irvine, A.E., Kennedy, R.J., and Bell, A.L. (1999). Increased apoptotic peripheral blood neutrophils in systemic lupus erythematosus: relations with disease activity, antibodies to double stranded DNA, and neutropenia. Ann. Rheum. Dis. *58*, 309–314.

Crotty, S. (2015). A brief history of T cell help to B cells. Nat. Rev. Immunol. *15*, 185–189.

DeBerardinis, R.J., Lum, J.J., Hatzivassiliou, G., and Thompson, C.B. (2008). The Biology of Cancer: Metabolic Reprogramming Fuels Cell Growth and Proliferation. Cell Metab. *7*, 11–20.

Drochmans, P. (1962). Morphologie du glycogène: Etude au microscope électronique de colorations négatives du glycogène particulaire. J. Ultrastruct. Res. *6*, 141–163.

Dumitru, C., Kabat, A.M., and Maloy, K.J. (2018). Metabolic Adaptations of CD4+ T Cells in Inflammatory Disease. Front. Immunol. *9*, 540. doi: 10.3389/fimmu.2018.00540

Eiraku, N., Hingorani, R., Ijichi, S., Machigashira, K., Gregersen, P.K., Monteiro, J., Usuku, K., Yashiki, S., Sonoda, S., Osame, M., et al. (1998). Clonal Expansion Within CD4+ and CD8+ T Cell Subsets in Human T Lymphotropic Virus Type I-Infected Individuals. J. Immunol. *161*, 6674–6680.

Erbel, C., Akhavanpoor, M., Okuyucu, D., Wangler, S., Dietz, A., Zhao, L., Stellos, K., Little, K.M., Lasitschka, F., Doesch, A., et al. (2014). IL-17A Influences Essential Functions of the Monocyte/Macrophage Lineage and Is Involved in Advanced Murine and Human Atherosclerosis. J. Immunol. *193*, 4344–4355.

Esensten, J.H., Helou, Y.A., Chopra, G., Weiss, A., and Bluestone, J.A. (2016). CD28 Costimulation: From Mechanism to Therapy. Immunity *44*, 973–988.

Fadista, J., Vikman, P., Laakso, E.O., Mollet, I.G., Esguerra, J.L., Taneera, J., Storm, P., Osmark, P., Ladenvall, C., Prasad, R.B., et al. (2014). Global genomic and transcriptomic

analysis of human pancreatic islets reveals novel genes influencing glucose metabolism. Proc. Natl. Acad. Sci. *111*, 13924–13929.

Fischer, K., Hoffmann, P., Voelkl, S., Meidenbauer, N., Ammer, J., Edinger, M., Gottfried, E., Schwarz, S., Rothe, G., Hoves, S., et al. (2007). Inhibitory effect of tumor cell–derived lactic acid on human T cells. Blood *109*, 3812–3819.

Franciszkiewicz, K., Boissonnas, A., Boutet, M., Combadiere, C., and Mami-Chouaib, F. (2012). Role of Chemokines and Chemokine Receptors in Shaping the Effector Phase of the Antitumor Immune Response. Cancer Res. *72*, 6325–6332.

Frauwirth, K.A., Riley, J.L., Harris, M.H., Parry, R.V., Rathmell, J.C., Plas, D.R., Elstrom, R.L., June, C.H., and Thompson, C.B. (2002). The CD28 Signaling Pathway Regulates Glucose Metabolism. Immunity *16*, 769–777.

Fu, J., Baines, K.J., Wood, L.G., and Gibson, P.G. (2013). Systemic Inflammation Is Associated with Differential Gene Expression and Airway Neutrophilia in Asthma. OMICS J. Integr. Biol. *17*, 187–199.

Gate, R.E., Cheng, C.S., Aiden, A.P., Siba, A., Tabaka, M., Lituiev, D., Machol, I., Gordon, M.G., Subramaniam, M., Shamim, M., et al. (2018). Genetic determinants of co-accessible chromatin regions in activated T cells across humans. Nat. Genet. *50*, 1140.

Goldsmith, E., Sprang, S., and Fletterick, R. (1982). Structure of maltoheptaose by difference Fourier methods and a model for glycogen. J. Mol. Biol. *156*, 411–427.

Greiner, E.F., Guppy, M., and Brand, K. (1994). Glucose is essential for proliferation and the glycolytic enzyme induction that provokes a transition to glycolytic energy production. J. Biol. Chem. *269*, 31484–31490.

Grist, J.T., Jarvis, L.B., Georgieva, Z., Thompson, S., Kaur Sandhu, H., Burling, K., Clarke, A., Jackson, S., Wills, M., Gallagher, F.A., et al. (2018). Extracellular Lactate: A Novel Measure of T Cell Proliferation. J. Immunol. Author Choice *200*, 1220–1226.

Güemes, M., Rahman, S.A., and Hussain, K. (2016). What is a normal blood glucose? Arch. Dis. Child. *101*, 569–574.

Hagemans, M.L.C., Stigter, R.L., van Capelle, C.I., van der Beek, N.A.M.E., Winkel, L.P.F., van Vliet, L., Hop, W.C.J., Reuser, A.J.J., Beishuizen, A., and van der Ploeg, A.T. (2010). PAS-positive lymphocyte vacuoles can be used as diagnostic screening test for Pompe disease. J. Inherit. Metab. Dis. *33*, 133–139.

Hayhoe, F.G.J., and Quaglino, D. (1965). Autoradiographic Investigations of RNA and DNA Metabolism of Human Leucocytes Cultured with Phytohæmagglutinin ; Uridine-5-3h as a Specific Precursor of RNA. Nature *205*, 151–154.

Hedeskov, C.J. (1968). Early effects of phytohaemagglutinin on glucose metabolism of normal human lymphocytes. Biochem. J. *110*, 373–380.

Heiden, M.G.V., Cantley, L.C., and Thompson, C.B. (2009). Understanding the Warburg Effect: The Metabolic Requirements of Cell Proliferation. Science *324*, 1029–1033.

Hertz, L., and Chen, Y. (2018). Glycogenolysis, an Astrocyte-Specific Reaction, is Essential for Both Astrocytic and Neuronal Activities Involved in Learning. Neuroscience *370*, 27–36.

Horvat, A., Vardjan, N., and Zorec, R. (2017). Targeting Astrocytes for Treating Neurological Disorders: Carbon Monoxide and Noradrenaline-Induced Increase in Lactate. Curr. Pharm. Des. *23*, 4969–4978.

Iritani, B.M., Delrow, J., Grandori, C., Gomez, I., Klacking, M., Carlos, L.S., and Eisenman, R.N. (2002). Modulation of T-lymphocyte development, growth and cell size by the Myc antagonist and transcriptional repressor Mad1. EMBO J. *21*, 4820–4830.

Jacobs, S.R., Herman, C.E., MacIver, N.J., Wofford, J.A., Wieman, H.L., Hammen, J.J., and Rathmell, J.C. (2008). Glucose Uptake Is Limiting in T Cell Activation and Requires CD28-Mediated Akt-Dependent and Independent Pathways. J. Immunol. *180*, 4476–4486.

Jones, R.V., Goffi, G.P., and Hutt, M.S.R. (1962). Lymphocyte glycogen content in various diseases. J. Clin. Pathol. *15*, 36–39.

Kamphorst, A.O., Wieland, A., Nasti, T., Yang, S., Zhang, R., Barber, D.L., Konieczny, B.T., Daugherty, C.Z., Koenig, L., Yu, K., et al. (2017). Rescue of exhausted CD8 T cells by PD-1–targeted therapies is CD28-dependent. Science *355*, 1423–1427.

Klabunde, T., Wendt, K.U., Kadereit, D., Brachvogel, V., Burger, H.-J., Herling, A.W., Oikonomakos, N.G., Kosmopoulou, M.N., Schmoll, D., Sarubbi, E., et al. (2005). Acyl ureas as human liver glycogen phosphorylase inhibitors for the treatment of type 2 diabetes. J. Med. Chem. *48*, 6178–6193.

Klein Geltink, R.I., Kyle, R.L., and Pearce, E.L. (2018). Unraveling the Complex Interplay Between T Cell Metabolism and Function. Annu. Rev. Immunol. *36*, 461–488.

Kleiveland, C.R. (2015). Peripheral Blood Mononuclear Cells. In The Impact of Food Bioactives on Health: In Vitro and Ex Vivo Models, K. Verhoeckx, P. Cotter, I. López-Expósito, C. Kleiveland, T. Lea, A. Mackie, T. Requena, D. Swiatecka, and H. Wichers, eds. (Cham (CH): Springer), pp. 161–167.

Komori, H.K., Hart, T., LaMere, S.A., Chew, P.V., and Salomon, D.R. (2015). Defining CD4 T Cell Memory by the Epigenetic Landscape of CpG DNA Methylation. J. Immunol. *194*, 1565–1579.

Kündig, T.M., Shahinian, A., Kawai, K., Mittrücker, H.-W., Sebzda, E., Bachmann, M.F., Mak, T.W., and Ohashi, P.S. (1996). Duration of TCR Stimulation Determines Costimulatory Requirement of T Cells. Immunity *5*, 41–52.

Kurrer, M.O., Pakala, S.V., Hanson, H.L., and Katz, J.D. (1997). β cell apoptosis in T cell-mediated autoimmune diabetes. Proc. Natl. Acad. Sci. *94*, 213–218.

Leder, L.D., and Donhuijsen, K. (1978). PAS-positive lymphatic cells in angioimmunoblastic lymphadenopathy. Klin. Wochenschr. *56*, 225–227.

Linsley, P.S., Greene, J.L., Tan, P., Bradshaw, J., Ledbetter, J.A., Anasetti, C., and Damle, N.K. (1992). Coexpression and functional cooperation of CTLA-4 and CD28 on activated T lymphocytes. J. Exp. Med. *176*, 1595–1604.

Lunt, S.Y., and Vander Heiden, M.G. (2011). Aerobic Glycolysis: Meeting the Metabolic Requirements of Cell Proliferation. Annu. Rev. Cell Dev. Biol. *27*, 441–464.

Ma, R., Ji, T., Zhang, H., Dong, W., Chen, X., Xu, P., Chen, D., Liang, X., Yin, X., Liu, Y., et al. (2018). A Pck1-directed glycogen metabolic program regulates formation and maintenance of memory CD8+ T cells. Nat. Cell Biol. *20*, 21–27.

Macintyre, A., Gerriets, V., Nichols, A., Michalek, R., Rudolph, M., Deoliveira, D., and Rathmell, J. (2014). The Glucose Transporter Glut1 Is Selectively Essential for CD4 T Cell Activation and Effector Function. Cell Metab. *20*, 61–72.

Magistretti, P.J., and Allaman, I. (2018). Lactate in the brain: from metabolic end-product to signalling molecule. Nat. Rev. Neurosci. *19*, 235–249.

McKinney, E.F., and Smith, K.G.C. (2018). Metabolic exhaustion in infection, cancer and autoimmunity. Nat. Immunol. *19*, 213–221.

Menk, A.V., Scharping, N.E., Moreci, R.S., Zeng, X., Guy, C., Salvatore, S., Bae, H., Xie, J., Young, H.A., Wendell, S.G., et al. (2018). Early TCR Signaling Induces Rapid Aerobic Glycolysis Enabling Distinct Acute T Cell Effector Functions. Cell Rep. *22*, 1509–1521.

Modiano, J.F., Domenico, J., Szepesi, A., Lucas, J.J., and Gelfand, E.W. (1994). Differential requirements for interleukin-2 distinguish the expression and activity of the cyclin-dependent kinases Cdk4 and Cdk2 in human T cells. J. Biol. Chem. *269*, 32972–32978.

Moore, C.S., Cui, Q.-L., Warsi, N.M., Durafourt, B.A., Zorko, N., Owen, D.R., Antel, J.P., and Bar-Or, A. (2015). Direct and Indirect Effects of Immune and Central Nervous System–Resident Cells on Human Oligodendrocyte Progenitor Cell Differentiation. J. Immunol. *194*, 761–772.

Newman, L.A., Korol, D.L., and Gold, P.E. (2011). Lactate Produced by Glycogenolysis in Astrocytes Regulates Memory Processing. PLOS ONE *6*, e28427.

Pascarella, A., Terracciano, C., Farina, O., Lombardi, L., Esposito, T., Napolitano, F., Franzese, G., Panella, G., Tuccillo, F., Marca, G. la, et al. (2018). Vacuolated PAS-positive lymphocytes as an hallmark of Pompe disease and other myopathies related to impaired autophagy. J. Cell. Physiol. *233*, 5829–5837.

Pennock, N.D., White, J.T., Cross, E.W., Cheney, E.E., Tamburini, B.A., and Kedl, R.M. (2013). T cell responses: naïve to memory and everything in between. Adv. Physiol. Educ. *37*, 273–283.

58

Quaglino, D., Hayhoe, F.G.J., and Flemans, R.J. (1962). Cytochemical observations on the effect of phytohaemagglutinin in short-term tissue cultures. Nature *196*, 338–340.

Quaglino, D., Cowling, D.C., and Hayhoe, F.G.J. (1964). Cytochemical and Autoradiographic Studies on Normal and Leukaemic Cells in Short-Term Tissue Cultures. Br. J. Haematol. *10*, 417–436.

Rashida Gnanaprakasam, J.N., Wu, R., and Wang, R. (2018). Metabolic Reprogramming in Modulating T Cell Reactive Oxygen Species Generation and Antioxidant Capacity. Front. Immunol. *9*, 1075. doi: 10.3389/fimmu.2018.01075

Rathmell, J.C., Elstrom, R.L., Cinalli, R.M., and Thompson, C.B. (2003). Activated Akt promotes increased resting T cell size, CD28-independent T cell growth, and development of autoimmunity and lymphoma. Eur. J. Immunol. *33*, 2223–2232.

Roach, J.C., Glusman, G., Rowen, L., Kaur, A., Purcell, M.K., Smith, K.D., Hood, L.E., and Aderem, A. (2005). The evolution of vertebrate Toll-like receptors. Proc. Natl. Acad. Sci. *102*, 9577–9582.

Roach, P.J., Depaoli-Roach, A.A., Hurley, T.D., and Tagliabracci, V.S. (2012). Glycogen and its metabolism: some new developments and old themes. Biochem. J. *441*, 763–787.

Robinson, P.J. (1992). Differential stimulation of protein kinase C activity by phorbol ester or calcium/phosphatidylserine in vitro and in intact synaptosomes. J. Biol. Chem. *267*, 21637–21644.

Sadiku, P., Willson, J.A., Dickinson, R.S., Murphy, F., Harris, A.J., Lewis, A., Sammut, D., Mirchandani, A.S., Ryan, E., Watts, E.R., et al. (2017). Prolyl hydroxylase 2 inactivation enhances glycogen storage and promotes excessive neutrophilic responses. J. Clin. Invest. *127*, 3407–3420.

Salou, M., Nicol, B., Garcia, A., and Laplaud, D.-A. (2015). Involvement of CD8+ T Cells in Multiple Sclerosis. Front. Immunol. *6*, 604. doi: 10.3389/fimmu.2015.00604

Saparov, A., Wagner, F., Zheng, R., and Weaver, C. (1999). Interleukin-2 Expression by a Subpopulation of Primary T Cells Is Linked to Enhanced Memory/Effector Function. Immunity *11*, 271–280.

Savtchouk, I., and Volterra, A. (2018). Gliotransmission: Beyond Black-and-White. J. Neurosci. *38*, 14–25.

Smith-Garvin, J.E., Koretzky, G.A., and Jordan, M.S. (2009). T cell activation. Annu. Rev. Immunol. *27*, 591–619.

Snapper, C.M., Zelazowski, P., Rosas, F.R., Kehry, M.R., Tian, M., Baltimore, D., and Sha, W.C. (1996). B cells from p50/NF-kappa B knockout mice have selective defects in proliferation, differentiation, germ-line CH transcription, and Ig class switching. J. Immunol. *156*, 183–191.

van Stipdonk, M.J.B., Hardenberg, G., Bijker, M.S., Lemmens, E.E., Droin, N.M., Green, D.R., and Schoenberger, S.P. (2003). Dynamic programming of CD8$^+$ T lymphocyte responses. Nat. Immunol. *4*, 361–365.

Stopnicki, B., Blain, M., Cui, Q.-L., Kennedy, T.E., Antel, J.P., Healy, L.M., and Darlington, P.J. (2019). Helper CD4 T cells expressing granzyme B cause glial fibrillary acidic protein fragmentation in astrocytes in an MHCII-independent manner. Glia 582–593.

Suzuki, A., Stern, S.A., Bozdagi, O., Huntley, G.W., Walker, R.H., Magistretti, P.J., and Alberini, C.M. (2011). Astrocyte-neuron lactate transport is required for long-term memory formation. Cell *144*, 810–823.

Tabatabaei Shafiei, M. (2016). The Effect of Immune Cell Activation on Glycogen Storage in the Context of a Nutrient Rich Microenvironment. Masters thesis. Concordia University.

Tabatabaei Shafiei, M., Gonczi, C.M.C., Rahman, M.S., East, A., François, J., and Darlington, P.J. (2014). Detecting Glycogen in Peripheral Blood Mononuclear Cells with Periodic Acid Schiff Staining. JoVE J. Vis. Exp. e52199–e52199.

Thwe, P.M., Pelgrom, L., Cooper, R., Beauchamp, S., Reisz, J.A., D'Alessandro, A., Everts, B., and Amiel, E. (2017). Cell-Intrinsic Glycogen Metabolism Supports Early Glycolytic Reprogramming Required for Dendritic Cell Immune Responses. Cell Metab. *26*, 558-567.e5.

Waitt, A.E., Reed, L., Ransom, B.R., and Brown, A.M. (2017). Emerging Roles for Glycogen in the CNS. Front. Mol. Neurosci. *10*, 73. doi: 10.3389/fnmol.2017.00073

Wang, R., Dillon, C.P., Shi, L.Z., Milasta, S., Carter, R., Finkelstein, D., McCormick, L.L., Fitzgerald, P., Chi, H., Munger, J., et al. (2011). The Transcription Factor Myc Controls Metabolic Reprogramming upon T Lymphocyte Activation. Immunity *35*, 871–882.

Weinhouse, S., Warburg, O., Burk, D., and Schade, A.L. (1956). On Respiratory Impairment in Cancer Cells. Science *124*, 267–272.

Wipke, B.T., and Allen, P.M. (2001). Essential Role of Neutrophils in the Initiation and Progression of a Murine Model of Rheumatoid Arthritis. J. Immunol. *167*, 1601–1608.

Zhang, Y., Chen, K., Sloan, S.A., Bennett, M.L., Scholze, A.R., O'Keeffe, S., Phatnani, H.P., Guarnieri, P., Caneda, C., Ruderisch, N., et al. (2014). An RNA-Sequencing Transcriptome and Splicing Database of Glia, Neurons, and Vascular Cells of the Cerebral Cortex. J. Neurosci. *34*, 11929–11947.

Zhao, Y., Zhang, Q., Shao, X., Ouyang, L., Wang, X., Zhu, K., and Chen, L. (2017). Decreased Glycogen Content Might Contribute to Chronic Stress-Induced Atrophy of Hippocampal Astrocyte volume and Depression-like Behavior in Rats. Sci. Rep. *7*.

Ziegler, S.F., Ramsdell, F., Hjerrild, K.A., Armitage, R.J., Grabstein, K.H., Hennen, K.B., Farrah, T., Fanslow, W.C., Shevach, E.M., and Alderson, M.R. (1993). Molecular

characterization of the early activation antigen CD69: A type II membrane glycoprotein related to a family of natural killer cell activation antigens. Eur. J. Immunol. *23*, 1643–1648.

APPENDIX

Formulas

$$\% \, Viability = \left(\frac{Total \; cell \; count - Dead \; cells}{Total \; cell \; count} \right) \times 100$$

Formula 1 – Calculation for % viability through trypan counting.

As explained in the methods section, trypan solution was added in a 1:1 ratio with live cells. Cells that have died will take up the trypan solution and will appear blue and opaque. The number of dead cells was subtracted from the total number of cells counted and then divided by the total number of cells counted.

$$RPKM = \frac{10^9 \times C}{N \times L}$$

Formula 2 – RPKM calculation.

For reporting results as RPKM, calculations attempt to normalize for sequencing depth and gene length. The first step is to normalize for the number of reads per gene (C). Then, divide the total number of reads for the gene (in kilobases) by the total mapped reads in the experiment (N) multiplied by the exon length for that gene (L).

$$TPM = \frac{C_i}{L_i} \times \left(\frac{1}{\sum_j \frac{C_j}{L_j}} \right) \times 10^6$$

Formula 3 – TPM calculation.

TPM represents the relative number of RNA transcript (i) for every million RNA molecules in the experiment sample. This formula was carried out per gene. First the transcript expression value was normalized by counting the number of reads for a gene (C_i) and then, for that gene (i), the number of reads (C) was divided by the length of gene transcript (L_i). This output (Ci/Li) was multiplied by the inverse of the sum for all counts per base of all genes (Cj/Lj) then all multiplied by the scaling factor (10^6).

Supplemental figures

```
 1 if (roiManager("Count")>0){
 2     roiManager("Deselect");
 3     roiManager("Delete");
 4 }
 5 rename("Original");
 6 run("Duplicate...", "title=background");
 7 run("Subtract Background...", "rolling=200 light separate create");
 8 imageCalculator("Difference create", "Original","background");
 9 selectWindow("Result of Original");
10 run("Split Channels");
11 selectWindow("Result of Original (green)");
12 rename("green");
13 run("Duplicate...", " ");
14 run("Gaussian Blur...", "sigma=2");
15 setAutoThreshold("Yen dark");
16 run("Convert to Mask");
17 run("Watershed");
18 run("Analyze Particles...", "size=1500-Infinity pixel exclude clear add");
19 close();
20 selectWindow("green");
21 roiManager("Measure");
```

Supplemental Figure 1 – Fiji macro for cell area and signal intensity

The images contrast was enhanced, and the green channel was split out. The green channel has the most contrast and is why this channel was chosen. Next, the image was blurred to hide small artifacts such as cell debris. Lastly the macro told Fiji to threshold the image to find areas above 1500 pixels in size which we assumed were cells. Lastly, these areas were selected as regions of interest and measured on the grey scale for mean pixel intensity.
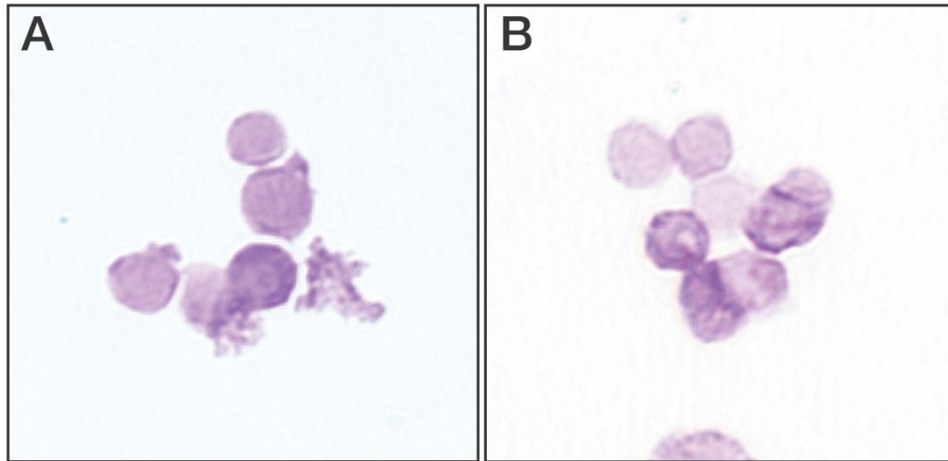
This figure depicts the pattern of PAS staining between 24- and 48-hour time points. Helper T cells that were stained at 24-hours after activation were consistently darker purple with diffuse staining throughout the inside of the cell whereas after 48-hours the stain concentrated into darker granules.
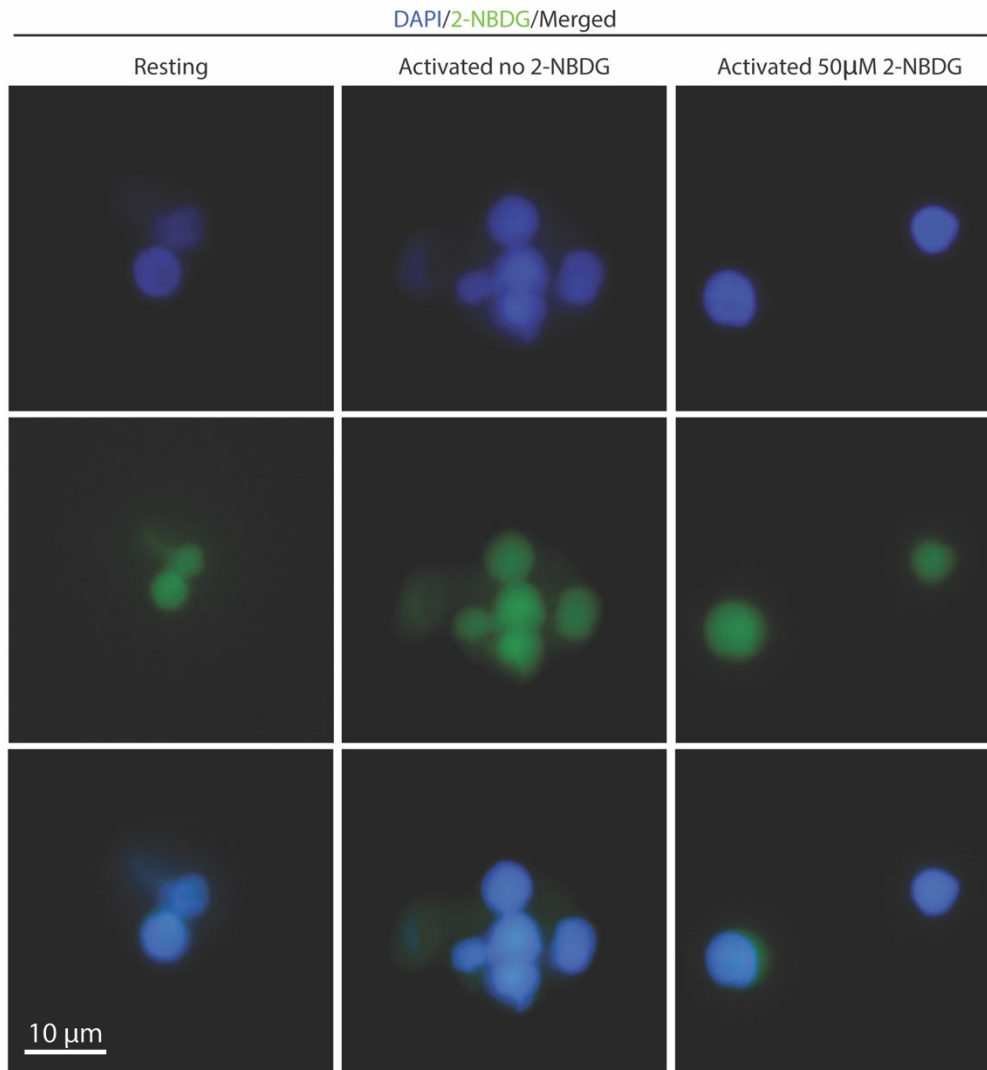
Supplemental Figure 3 – 2-NBDG in PBMCs

Immunofluorescent images of PBMCs show 2-NBDG (green) did not effectively form granules inside PBMCs. PBMCs seem to be auto-fluorescent and therefore 2-NBDG is an unreliable method for measuring glycogen. 2-NBDG signal (green) is observed in control conditions (no 2-NBDG). DAPI (blue) was used as a nuclear stain. Magnification = 60x